

## **Analyses of Near-Field and Near-Regional Signals from the Black Thunder Mine**

**Terrance G. Barker  
Keith L. McLaughlin**

**Maxwell Technologies, Inc.  
8888 Balboa Avenue  
San Diego, CA 92123-1506**

**February 1998**

**Final Report**

**10 August 95 - 9 August 97**

**Approved for public release; distribution unlimited**



**DEPARTMENT OF ENERGY  
Office of Nonproliferation and National Security  
WASHINGTON, DC 20585**



**AIR FORCE RESEARCH LABORATORY  
Space Vehicles Directorate  
29 Randolph Rd  
Hanscom AFB, MA 01731-3010**

19981016 027


SPONSORED BY  
Department of Energy  
Office of Non-Proliferation and National Security

MONITORED BY  
Air Force Research Laboratory  
CONTRACT No. F19628-95-C-0112

The views and ~~con~~clusions contained in this document are those of the authors and should not be interpreted as ~~re~~presenting the official policies, either express or implied, of the Air Force or U.S. Government.

This technical ~~re~~port has been reviewed and is approved for publication.

  
KATHARINE KADINSKY-CADE  
Contract Manager

  
CHARLES P. PIKE, Deputy Director  
Integration and Operations Division

This report has been reviewed by the ESD Public Affairs Office (PA) and is releasable to the National Technical Information Service (NTIS).

Qualified requestors may obtain copies from the Defense Technical Information Center. All others should apply to the National Technical Information Service.

If your address has changed, or you wish to be removed from the mailing list, or if the addressee is no longer employed by your organization, please notify AFRL/VSOS-IM, 29 Randolph Road, Hanscom AFB, MA 01731-3010. This will assist us in maintaining a current mailing list.

Do not return copies of the report unless contractual obligations or notices on a specific document requires that it be returned.

REPORT DOCUMENTATION PAGE			Form Approved OMB No. 0704-0188	
Public reporting burden for this collection of information is estimated to average 1 hour per response, including the time for reviewing instructions, searching existing data sources, gathering and maintaining the data needed, and completing and reviewing the collection of information. Send comments regarding this burden estimate or any other aspect of this collection of information, including suggestions for reducing this burden, to Washington Headquarters Services, Directorate for Information Operations and Reports, 1215 Jefferson Davis Highway, Suite 1204, Arlington VA 22202-4302, and to the Office of Management and Budget, Paperwork Reduction Project (0704-0188), Washington, DC 20503.				
1. AGENCY USE ONLY (Leave blank)		2. REPORT DATE February 1998	3. REPORT TYPE AND DATES COVERED Final (10 August 1995 - 9 August 1997)	
4. TITLE AND SUBTITLE Analysis of Near-Field and Near-Regional Signals from the Black Thunder Mine			5. FUNDING NUMBERS Contract No. F19628-95-C-0112 PE 6912OH PR DENN TA GM WU AV	
6. AUTHOR(S) Terrance G. Barker, Keith L. McLaughlin				
7. PERFORMING ORGANIZATION NAME(S) AND ADDRESS(ES) Maxwell Technologies, Inc. Federal Division 8888 Balboa Avenue San Diego, CA 92123-1506			8. PERFORMING ORGANIZATION REPORT NUMBER  MFD-DTR-98-15992	
9. SPONSORING/MONITORING AGENCY NAME(S) AND ADDRESS(ES) Air Force Research Laboratory 29 Randolph Road Hanscom AFB, MA 01731-3010 Contract Manager: Katharine Kadinsky-Cade/VSBS			10. SPONSORING/MONITORING AGENCY REPORT NUMBER  AFRL-VS-HA-TR-98-0033	
11. SUPPLEMENTARY NOTES This research was sponsored by the Department of Energy, Office of Non-Proliferation and National Security, Washington, DC 20585				
12a. DISTRIBUTION/AVAILABILITY STATEMENT  Approved for public release; distribution unlimited			12b. DISTRIBUTION CODE	
13. ABSTRACT (Maximum 200 words)  In this report we present analyses of seismic data recorded at the Black Thunder coal strip mine in the Powder River Basin of Wyoming. The data (collected by Stump <i>et al.</i> , 1996) are a set of recordings at distances of a few kilometers from mining activity at that mine. Our objective was to determine whether these near-field data revealed features of quarry blasting that were unique to that source type. In our previous annual report on this research contract (Barker <i>et al.</i> , 1997) and in Bonner <i>et al.</i> (1997), we described analyses of near-regional surface waves from a quarry in Texas. Their analyses used numerical simulations and predictions of the kinematic model in Barker <i>et al.</i> (1993) to interpret the dependence of amplitudes on azimuth in terms of quarry geometry and mass movement. Our objective in the current study was to apply these results to the recorded explosions at the Black Thunder mine. We find the following: <div style="text-align: right;">Continues . . .</div>				
14. SUBJECT TERMS  Seismic Test Ban Treaty Source Identification Quarry Blasts			15. NUMBER OF PAGES 52	
			16. PRICE CODE	
17. SECURITY CLASSIFICATION OF REPORT Unclassified	18. SECURITY CLASSIFICATION OF THIS PAGE Unclassified	19. SECURITY CLASSIFICATION OF ABSTRACT Unclassified	20. LIMITATION OF ABSTRACT  SAR	

**UNCLASSIFIED**

SECURITY CLASSIFICATION OF THIS PAGE

CLASSIFIED BY:

DECLASSIFIED ON:

13. ABSTRACT (Continued)

1. Ripple firing effectively low pass filters the signals, in agreement with previous studies. Since for the near-field signals at Black Thunder, the observed high frequency components of the signals are associated with P waves and the lower frequency signals are associated with surface waves (dominated by shear motion), ripple firing has the indirect effect of increasing the S/P ratio in the seismograms.
2. We observe no consistent differences between motions from cast blasts and coal shots, nor between cast shots in which the throw or strike of the bench is different. This is due to the dominance of ground motion due to explosions relative to that caused by mass movement, which is in turn is due to relative source coupling or propagation. Since differences in mass movement are the primary differences in the source mechanisms between coal and cast blasts, the dominance of the explosion component obscures the source mechanism.
3. Vertical and tangential near field ground motions (corrected for site response) from cast blasts are strongly enhanced normal to the bench in the direction of unmined land. We have no azimuthal coverage of a coal shot.

In addition to studies of near-field data, we analyzed near-regional data presented by Hedlin *et al.*, (1996). In the summer of 1996, IGPP/UCSD deployed five seismometers at ranges between 100 and 200 km from the Black Thunder mine, which augment the permanent regional stations RSSD and PDAR. After correcting for propagation, we have examined the data for dependence on azimuth and source location. The data are from shots in two pits that are perpendicular to each other and include a shot in which a fraction of the charges detonated simultaneously. The corrected ground motions show no azimuthal dependence on shot orientation.

## TABLE OF CONTENTS

Section	Page
1 Introduction .....	1
2 Experimental Setup, Mine Description and Description of Data.....	4
3 Effects of Ripple Firing .....	8
4 Radiation Patterns .....	11
5 Differences Due to Source Type .....	14
6 Black Thunder Mine Series: Regional Data .....	32
7 Conclusions .....	37
8 References .....	38

## FIGURES

Figure		Page
1	Locations of shots (circles) and recorders (triangles) relative to shot 167 .....	4
2	Vertical seismogram from shot 167 recorded at station R3 .....	7
3	Firing pattern time series for shots 167 and 174 .....	9
4	Time series from top to bottom are (1) the simultaneous coal shot 236 (2) coal shot 236 convolved with the firing pattern for cast blast 167, (3) cast blast 167 (4) the coal shot convolved with the firing pattern for cast blast 174, and (5) cast blast 174 .....	10
5	Polar radiation patterns of peak vertical amplitudes of the large cast blasts corrected for response computed from the Powder River Basin coda. ....	12
6	Polar radiation patterns of peak tangential amplitudes of the large cast blasts corrected for response computed from the Powder River Basin coda .....	12
7	Seismogram and spectrogram (vertical component) for cast blast 167 in the south pit, recorded at station R3 .....	14
8	Seismogram and spectrogram (vertical component) for cast blast 174 in the south pit, recorded at station R3 .....	15
9	Seismogram and spectrogram (vertical component) for coal shot 193 in the south pit, recorded at station R3 .....	15
10	Vertical seismograms for three cast blasts in the south pit, recorded at R3 .....	16
11	Vertical seismograms for three coal shots in the south pit, recorded at R3 .....	17
12	Narrow band envelope functions and S/P ratios (vertical component) for cast shots in the south pit at station R3 .....	18
13	Narrow band envelope functions and S/P ratios (vertical component) for cast shots in the south at station R3 .....	19

## FIGURES (continued)

Figure		Page
14	Vertical component seismograms from three coal shots in the south pit and one in the west pit at station R3 .....	20
15	Special amplitudes of the surface waves for the shots in this data set .....	22
16	Earth structure used in the calculation of synthetic seismograms .....	24
17	The spall and explosive contributions to the synthetic vertical motion at R3 for the shot 174 source model .....	25
18	Tangential synthetic and observed displacement seismograms from coal shot 236 at R3 .....	26
19	Vertical synthetic and observed displacement seismograms from coal shot 236 at R3 .....	27
20	Tangential synthetic and observed displacement seismograms from cast blast 167 at R3 .....	28
21	Vertical synthetic and observed displacement seismograms from cast blast 167 at R3 .....	29
22	Tangential synthetic and observed displacement seismograms from cast blast 174 at R3 .....	30
23	Vertical synthetic and observed displacement seismograms from cast blast 174 at R3 .....	31
24	Map showing Black Thunder mine and stations deployed by Hedlin, et al. (1996) .....	32
25	Shear velocity structure at four sites from the shot on Julian day 1996201 .....	33
26	Log of spectra at stations MNTA and SHNR .....	34
27	Log of spectra of South Pit shots 214 and 215 relative to North pit shot 201, at stations MNTA and SHNR .....	35
28	Radiation patterns of path corrected spectral amplitudes at 0.8 Hz for shots 201, 214 and 215 .....	36

## TABLES

Table		Page
1	Shot descriptions .....	5
2	Source-receiver matrix .....	6
3	Spectral slopes of the surface waves for the shots in this data set .....	21



## 1.0 Introduction

In this report we present analyses of seismic data recorded at the Black Thunder coal strip mine in the Powder River Basin of Wyoming. The data (collected by Stump *et al.*, 1996) are a set of recordings at distances of a few kilometers from mining activity at that mine. Our objective was to determine whether these near-field data revealed features of quarry blasting that were unique to that source type. All the mining activity involved explosions, of course, but they were designed to suit different purposes whose differences could potentially be used to isolate aspects of quarry blast sources. In this series were standard quarry cast blasts that were designed to fracture and cast material from a bench onto the mine floor. Another source type was the coal shot that was detonated in the mine floor. The purpose of coal shots is to fracture ("bulk") the coal prior to excavation and involves very little net movement of the fractured material. To reduce ground roll to neighboring areas and enhance fracturing, both of these shot types are ripple-fired. The data also include recordings of a coal shot which was not ripple-fired (all charges were detonated simultaneously), done by the mine operators at the request of the experimenters for the purpose of studying the effects of ripple-firing on seismic signals.

Each shot type, then, had an explosive component, with the ripple-fired shots having an extended source duration. The coal shots heaved the ground vertically (as can be seen in video recordings), so there should be a seismic force associated with the ballistic (spall) motion of the heaved material similar to that observed in nuclear explosions. Indeed, we approached the analysis assuming the coal shots could be modeled along the lines of an underburied nuclear explosion with an explosive component and spall component, as proposed by several authors (Day and McLaughlin, 1991, Barker *et al.*, 1993a, Taylor and Randall, 1989). Cast blasts involve mass movement that has both vertical and horizontal net displacement. Barker *et al.* (1993b), proposed a kinematic model of cast blasts that included vertical and horizontal net displacement, and this model provided the conceptual framework for studying the cast blast signals.

In addition to the three source types mentioned above, other source variables included bench location and throw direction. In our annual report on the first year of this research contract (Barker *et al.*, 1997) and in Bonner *et al.* (1996), we described analyses of near-regional surface waves from a quarry in Texas. Their analyses used numerical simulations and predictions of the kinematic model in Barker *et al.* (1993b) to interpret the dependence of amplitudes on azimuth in terms of quarry geometry and mass movement. Our objective in the current study was to apply these results to the recorded explosions at the Black Thunder mine.

In addition to studies of near-field data, we analyzed near-regional data presented by Hedlin *et al.*, (1996). In the summer of 1996, IGPP/UCSD deployed five seismometers at ranges between 100 and 200 km from the Black Thunder mine, which augment the permanent regional stations RSSD and PDAR. After correcting for propagation, we have examined the data for dependence on azimuth and source location. The data are from shots in two pits that are perpendicular to each other and include a shot

in which a fraction of the charges detonated simultaneously. The corrected ground motions show no azimuthal dependence on shot orientation.

Surficial sedimentary layers made analysis of signals at the Black Thunder mine difficult. Inspection of the seismograms shows that the ground motions are strongly influenced by local earth structure. Signals at 11 km have duration exceeding 25 seconds, which greatly exceeds the duration of ripple firing and ballistic motion of the material. Since structure is so important, and we have no independent measurements of seismic velocity, we have inferred a velocity model from the blast data. We began with kinematic models of the quarry blasts based on blast design. We computed synthetic seismograms from plane-layered earth models which were modified to match essential features of the observed seismograms. Having no absolute timing information, the features were the shape and duration of the signals. Comparison of the derived earth structure with recent borehole measurements give us confidence in the results.

A difficulty encountered in the interpretation of these data is a lack of statistical confidence. That is, rarely were shots of the same type in the same pit recorded on seismometers at the same place. Thus, we could not reliably observe the effects of varying one parameter while holding others fixed. The data we have are good quality, but logistical constraints on the experimenters limited the breadth of the data set (B. Stump and C. Pearson, private communication). Nevertheless, we proceeded with the analysis and make the following conclusions.

1. Ripple firing effectively low pass filters the signals, in agreement with previous studies. Since for the near-field signals at Black Thunder, the observed high frequency components of the signals are associated with P waves and the lower frequency signals are associated with surface waves (dominated by shear motion), ripple firing has the indirect effect of increasing the S/P ratio in the seismograms.
2. We observe no consistent differences between motions from cast blasts and ripple-fired coal shots. In our previous numerical studies under this contract (Barker *et al.*, 1997) and in field studies (Bonner *et al.* 1996), azimuthal variations due to throw or strike of the bench were predicted and observed. We observe no differences between cast shots at the Black Thunder mine in which the throw or strike of the bench is different. We examined differences in seismogram character, S/P ratio and spectral slope. The lack of differences is due to the dominance of ground motion caused by explosions relative to that caused by mass movement, which is in turn is due to relative source coupling or propagation. Since differences in mass movement are the primary differences in the source mechanisms between coal and cast blasts, the dominance of the explosion component obscures the source mechanism.
3. Vertical and tangential near field ground motions (corrected for site response) from cast blasts are strongly enhanced normal to the bench in the direction of unmined land. We have no azimuthal coverage of a coal shot.

4. In contrast to the results of our previous studies in Texas (Barker *et al.*, 1997, Bonner *et al.* 1996), near-regional ground motions (corrected for path) show no azimuthal dependence on shot orientation, presumably for the same reasons azimuthal variations are not observed in the near field data.

## 2.0 Experimental Setup, Mine Description and Description of Near-Field Data

Data from several shots in the South, West and Northeast Pits, described in Stump *et al.* (1996), were made available to us by Dr. Craig Pearson at LANL. The field layout is shown in Figure 1. Shot descriptions are given in Table 1. Descriptions of the sensors and experimental procedures can be found in Stump *et al.* (1996).

There are two main shot types in this data set: cast shots which are designed to move material from a bench to the floor of the mine and coal shots which fracture the material in the floor of the mine. Coal shots are meant to move material vertically only. Both these shots are ripple-fired. A third shot type is a simultaneous coal shot where all charges in this blast were detonated simultaneously. Mining operations have proceeded from north to south, and the land is reclaimed after coal is removed.

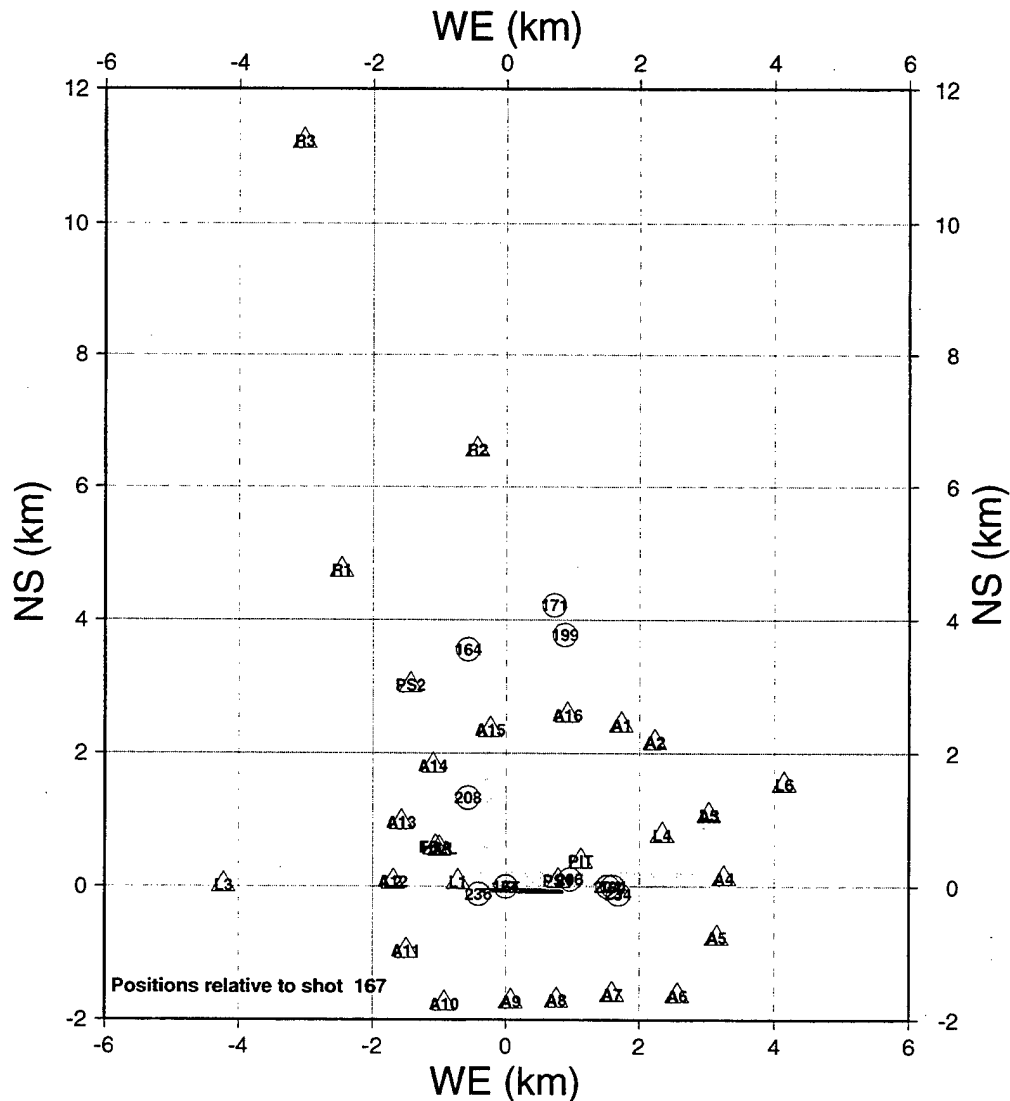


Figure 1. Locations of shots (circles) and recorders (triangles) relative to shot 167. The West and South Pits are shown as stippled areas.

Table 1. Shot descriptions.

shot	TYPE	PIT	W (kT)
s167	cast	S	4.41
s174	cast	S	1
s236	Simultaneous coal	S	0.002
s171	coal	NE	0.05
s184	coal	S	0.07
s193	cast	S	0.16
s199	cast	NE	1.66
s204	coal	S	0.16
s206	cast	S	1.55
s208	coal	W	0.08

A matrix showing source-receiver combinations for which we were provided data is displayed in Table 2. To isolate the effects of source and propagation on radiation patterns, distance dependence and seismogram attributes such as duration, and P to S ratio, we would ideally have data at multiple azimuths and distances from different shot types and different shot locations (pits). Of course, some degree of repeatability is useful. Although we were provided with a large amount of high quality data, they generally did not fulfill these requirements. The "A" stations (see Figure 1) form a ring around the center of the south pit at a radius of about 2 km. However, they were deployed for only two cast blasts in the South Pit and for no coal shots. The "R" stations, which form a line along a roughly NNW azimuth, recorded shots of each type and were useful for studying the effects of source type (although the shots were in different pits), but the line is obviously along only one azimuth.

By way of introduction to the nature of the near-field ground motions in this data set, we show in Figure 2 the vertical ground motions from shot 167 (see Table 1) recorded at station R3 at a distance of about 13 km and heading NNW from the shot. This figure illustrates several features of the signals typical of this data set. Perhaps the most striking feature is the duration of the signals, which is 25 to 30 seconds. Since the duration of the detonations and subsequent mass movement are only a few seconds, the length of the wave trains are due to propagation. As is discussed in Section 5, the long wave trains are surface waves with a dominant frequency of 1 Hz travelling in low velocity surficial layers. The higher frequency, earlier arriving signals are shallow P waves. In general, the surface waves are several times larger than the P waves.

Table 2. Source-receiver matrix (available data indicated by x's).

Shot receiver	s167	s174	s236	s171	s184	s193	s199	s204	s206	s208
A1	x	x								
A2	x	x								
A3	x	x								
A4	x	x								
A5	x	x		x						
A6	x	x	x	x	x	x	x	x	x	x
A7	x	x		x						
A8	x	x		x						
A9	x	x		x						
A10	x	x								
A11	x	x		x						
A12	x	x	x			x				
A13	x	x	x	x	x	x	x	x	x	x
A14	x	x								
A15	x	x								
A16	x			x						
R1	x	x	x	x	x		x	x	x	x
R2	x	x	x	x	x	x	x	x	x	x
R3	x	x	x	x	x	x	x	x	x	x
R4						x	x	x	x	x
R5						x	x			
R6						x	x			
R7						x	x			
R8						x	x			
R9						x	x			
R10						x	x			
R11							x			
R12				x		x				
L1										
L2	x	x	x	x		x				
L3				x						
L4										
L5	x	x		x						
L6			x							

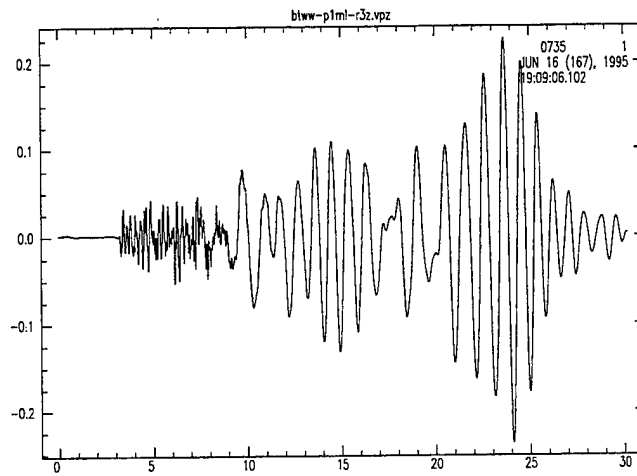


Figure 2. Vertical seismogram from shot 167 (see Table 1) recorded at station R3.

### 3.0 Effects of Ripple Firing

The recordings for which we have the most complete coverage are three South Pit shots. The shots are two large ripple-fired cast shots, and the simultaneous coal shot (see Table 1). Figure 1 shows the location of the pit (stippled area) at the time of these shots. Mining operations have proceeded from north to south, and the land is reclaimed after coal is removed. Thus, the highwall is on the south side of the pit. The cast blasts originated at nearly the same location, with shot 167 (4.7 million lbs.) propagating to the right, ending at the edge of the pit, and shot 174 (2.3 million lbs.) propagating to the left. The material was thrown to the NE by shot 167 and to the NW by shot 174. The coal shot (day 236) is west of shot 167 near the western end of the South Pit.

The duration of the signals is affected by the firing patterns, albeit to a lesser degree than by propagation. We can examine the effects of source duration by convolving the firing sequences of the cast blasts with the simultaneous coal shot. That is, we treat the simultaneous coal shot as a propagation Green's function. The shot durations (Figure 3) are several seconds. Figure 4 shows the results of the convolutions. From Figure 4, we see that the effects of the firing pattern time history are to (1) increase the duration of the signals and (2) increase the ratio of peak surface wave amplitude to P wave. The surface-to-P-wave-ratios of the convolutions and of the simultaneous coal shot are smaller than those of the cast blasts. We note that a fairly good fit to the cast blast records was achieved using the coal shot as a Green's function, which indicates that large mass movements affect the signals less than the explosive component.



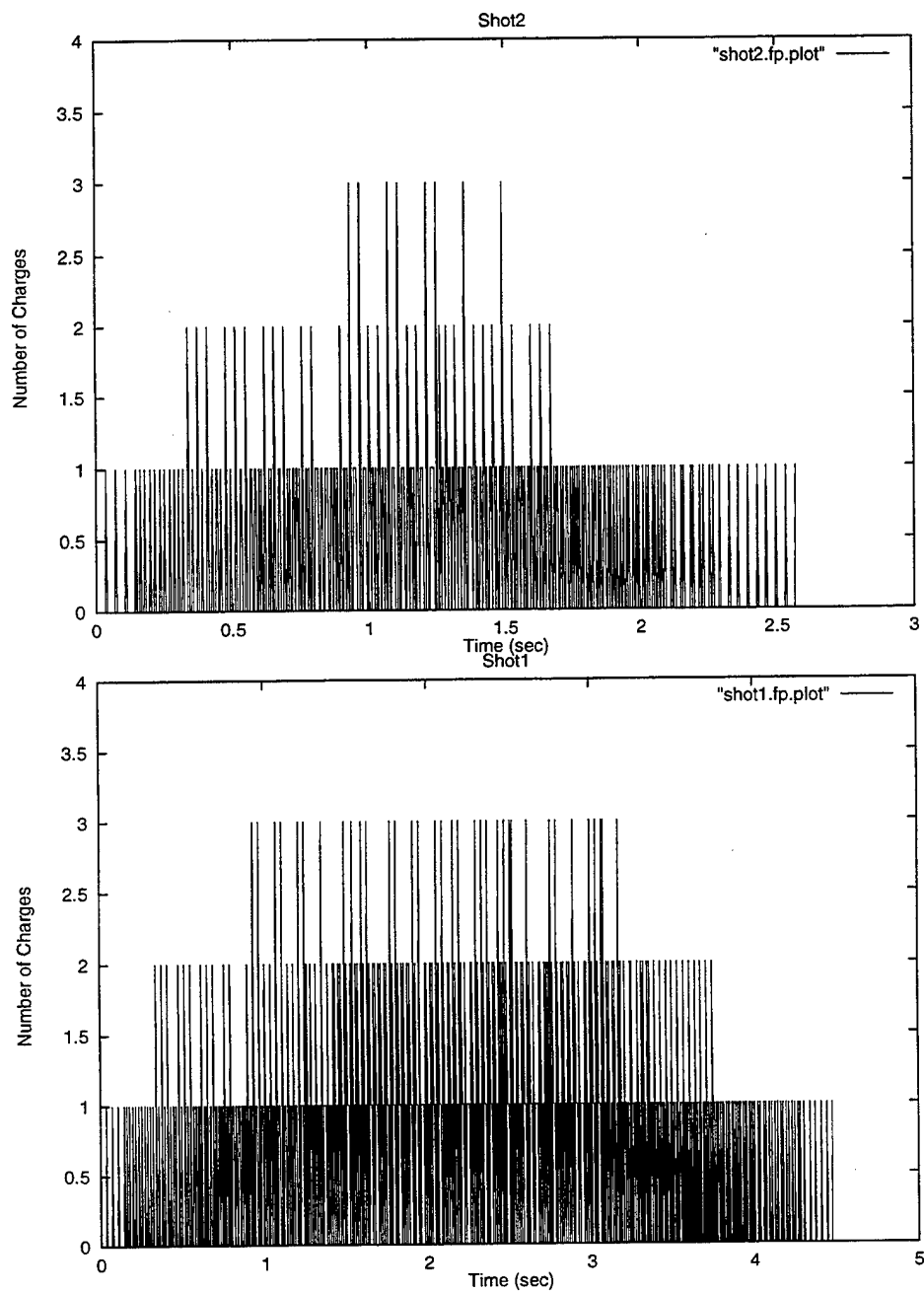


Figure 3. Firing pattern time series for shots 167 (above) and 174 (below).

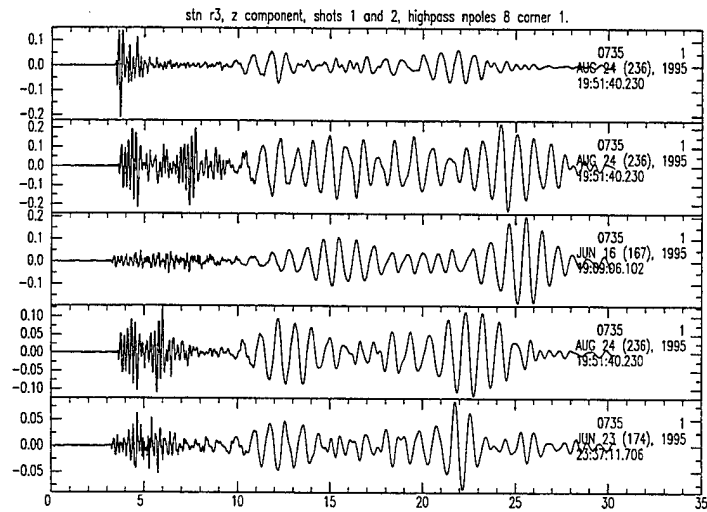


Figure 4. Time series from top to bottom are (1) the simultaneous coal shot 236, (2) coal shot 236 convolved with the firing pattern for cast blast 167, (3) cast blast 167, (4) the coal shot convolved with the firing pattern for cast blast 174, and (5) cast blast 174.

## 4.0 Radiation Patterns

We now consider the radiation patterns from these shots using recordings at the "A" stations (Figure 1), which encircle the shots. The response at the "A" stations is strongly influenced by the local site conditions, in particular, whether the site was on unmined or reclaimed land (Barker *et al.*, 1996). In our previous work, we used the coda of signals from the shots themselves to estimate site responses. This gave site corrections and amplitudes corrected for site response which were substantially different for the two cast blasts, indicating that the responses were not good estimates. We show in the following the results of using the coda of signals from distant shots in the Powder River Basin to estimate site response. The site responses using the powder River Basin shots gave results that were quite consistent from shot to shot. Figures 5 and 6 show radiation patterns of peak amplitudes of the large cast blasts, corrected for response computed from the Powder River Basin coda. Peak amplitudes are associated with surface waves with frequencies near one Hz (e.g., the energy arriving between 10 and 30 seconds in Figure 2).

Mining operations at Black Thunder have progressed in a generally north to south direction. After mining, the land is filled, or reclaimed. Stations A1 through A5 and A15 are on reclaimed land and stations A6 through A14 are on unmined land. Uncorrected peak motions are larger on unmined land and smaller on reclaimed land (Barker *et al.*, 1996), while the converse is true for corrected amplitudes. In light of the complexities of the shots and the mine setting, the patterns are quite consistent. Both components of motion show strong amplification to the south. Amplification of motion behind the bench is consistent with previous studies. The radiation patterns appear to be insensitive to the throw of materials by the explosions.

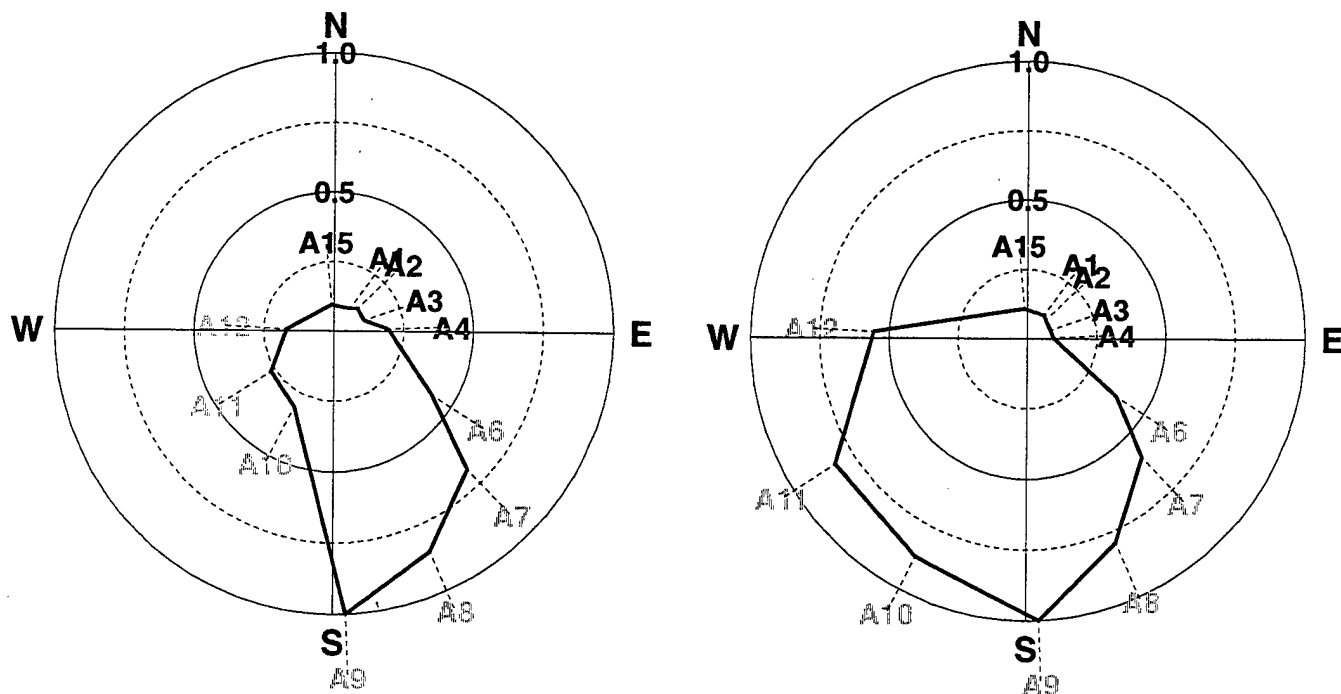


Figure 5. Polar radiation patterns of peak vertical amplitudes of the large cast blasts (167 on left, 174 on the right), corrected for response computed from the Powder River Basin coda. Bold station names are on reclaimed land and faded station names are on unmined land.

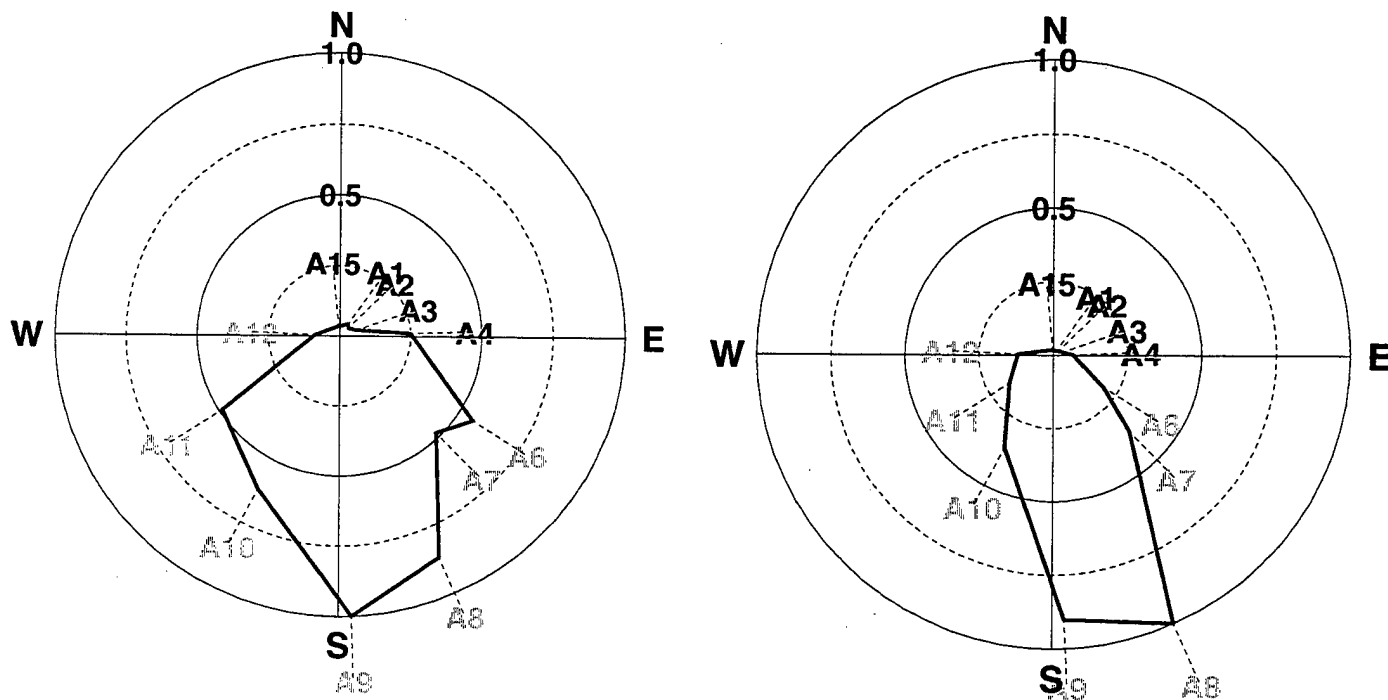


Figure 6. Polar radiation patterns of peak tangential amplitudes of the large cast blasts (167 on left, 174 on the right), corrected for response computed from the Powder River Basin coda. Bold station names are on reclaimed land and faded station names are on unmined land.

The equivalent force model predicts amplification of SH motion normal to the throw of spalled material and amplification of SV motion parallel to the throw. The explosive component and the vertical movement of material would contribute isotropic motions only in the vertical direction. Recall that the direction of throw for shots 167 and 174 differ by  $90^{\circ}$ . The observed radiation patterns do not reflect this difference.

Bonner and Goforth (1995) noticed that the character of seismograms from a central Texas quarry were correlated with the orientation of the active quarry face as the quarry operations migrated within the quarry. In a subsequent study with good azimuthal coverage of a few blasts at the Chemline quarry, Bonner *et al.* (1996) inferred Rg radiation patterns from phase matched filtered Rg. They found Rg was enhanced behind the bench and attenuated for paths crossing the quarry floor. Delitsyne *et al.* (1996) studied intermediate period Love waves from quarry blasts in Siberia. They found that the polarity of Love waves on opposing quarry faces were reversed and that blasts in the floor of the quarry produced small Love waves compared to Rg. They concluded that the Love wave polarity reversals and amplitude dependence were consistent with a spall mechanism for the generation of Love waves from the quarry faces and opening of a vertical tension crack for blasts in the quarry floor as suggested by the master crack model of Konya and Walter (1990).

Two possible mechanisms for such non-isotropic radiation are 1) the lateral throw of spalled material, and 2) the presence of the topographic bench in the quarry (Barker *et al.*, 1993a,b; and McLaughlin *et al.*, 1994). The spall of material can be modeled by vertical and horizontal forces applied to the free surface with time functions proportional to the derivative of the momentum of the spalled material.

Barker *et al.* (1996) modeled the Chemline data (Bonner *et al.*, 1996) using finite difference computations to account for the quarry geometry and synthetic seismogram calculations using the equivalent force model in Barker *et al.*, (1993a). The radiation patterns of Love waves in the numerical simulations exhibit minima at azimuths perpendicular to the face of the quarry and maxima parallel to the quarry faces. Rayleigh waves (Rg) are enhanced behind the quarry face. The Love wave (SH or transverse) radiation patterns are similar to the observed radiation patterns at the Chemline quarry. However, the observed radiation patterns in Rg cannot be produced by the topographic bench alone. The observed enhancement of Rg behind the bench is much larger than can be explained by the topographic effects. This is also the case for the Black Thunder data.

## 5.0 Differences Due to Source Type

In the following, we explore the differences between signals from the two source types: coal shot and cast blast. We begin with qualitative observations in the time and frequency domain. We show a seismogram and spectrogram in Figures 7 through 9 for cast blasts 167 and 174 and coal shot 193, recorded at station R3. Both shots were in the south pit. We will focus on station R3 in this section of the report, but the conclusions reached here apply to other stations. Each of the seismograms can be characterized by a small, early arriving, broad band P wave train in the first 5 seconds of the record, followed by a larger, narrow band (1 to 2 Hz) surface wave whose duration is about 20 seconds. The largest motions occur at different times for each shot. There appear to be spectral nulls on the coal shot spectrogram between 10 and 12 seconds at about 5 Hz intervals. Generally speaking, however, the differences between the signals from the two shot types are as great as the differences between the signals from the two cast blasts. This comment applies to the radial and tangential components as well.

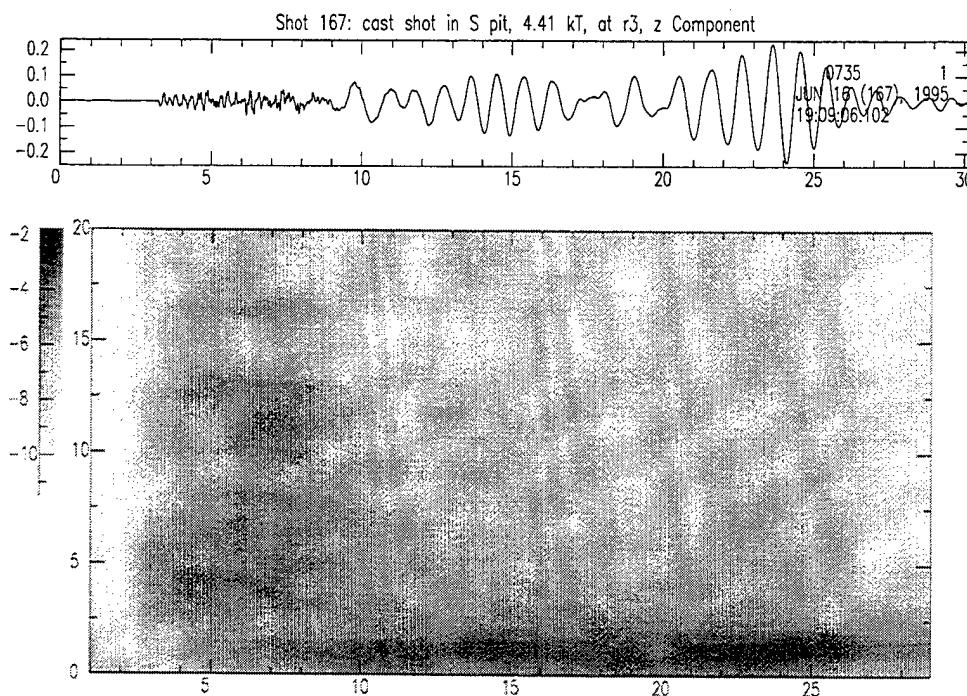


Figure 7. Seismogram and spectrogram (vertical component) for cast blast 167 in the south pit, recorded at station R3. Amplitude scale of the spectrogram (on the left) is in log units.

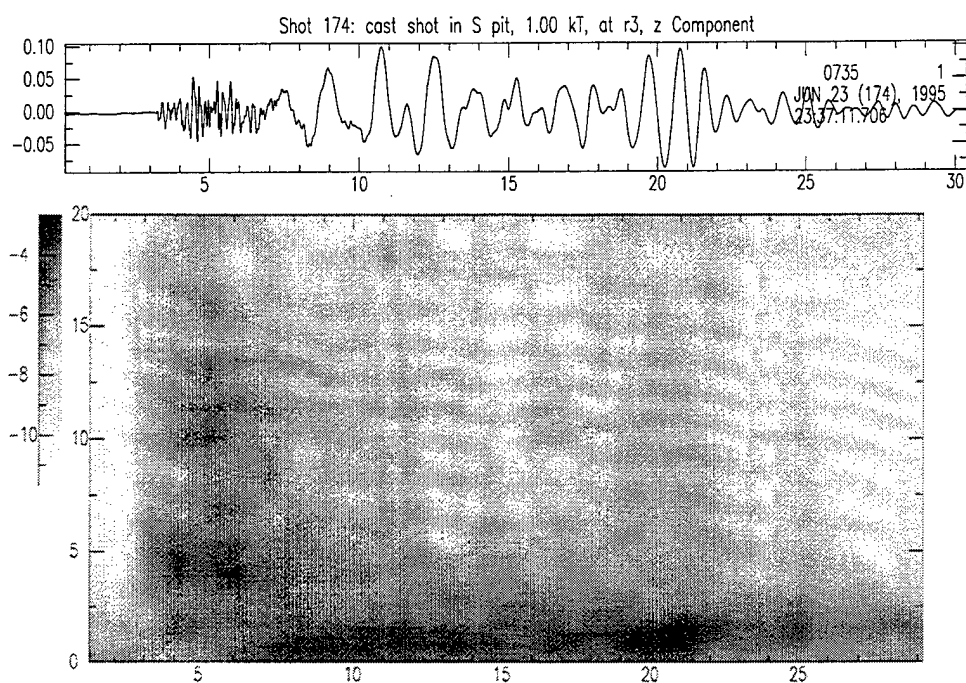


Figure 8. Seismogram and spectrogram (vertical component) for cast blast 174 in the south pit, recorded at station R3.

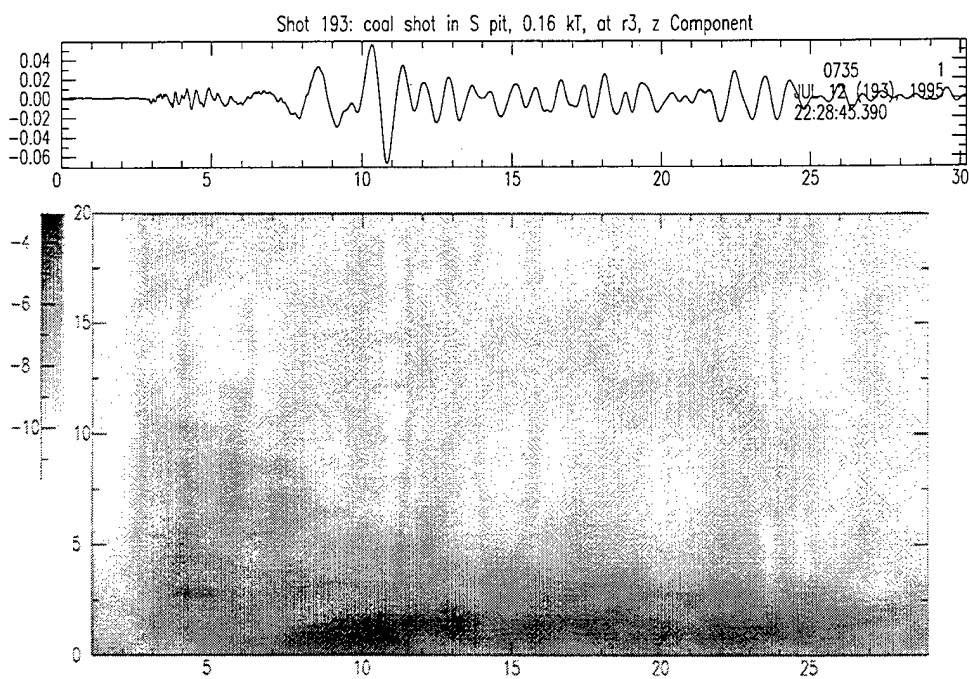


Figure 9. Seismogram and spectrogram (vertical component) for coal shot 193 in the south pit, recorded at station R3.

The ratio of shear to compressional energy in a regional signal is a feature often studied as a discriminant. In the following, we examine this ratio in the Black Thunder near field data. Again, we focus on blasts occurring in the south pit, recorded at station R3. Seismograms for three cast blasts are shown in Figure 10, and for three coal shots in Figure 11.

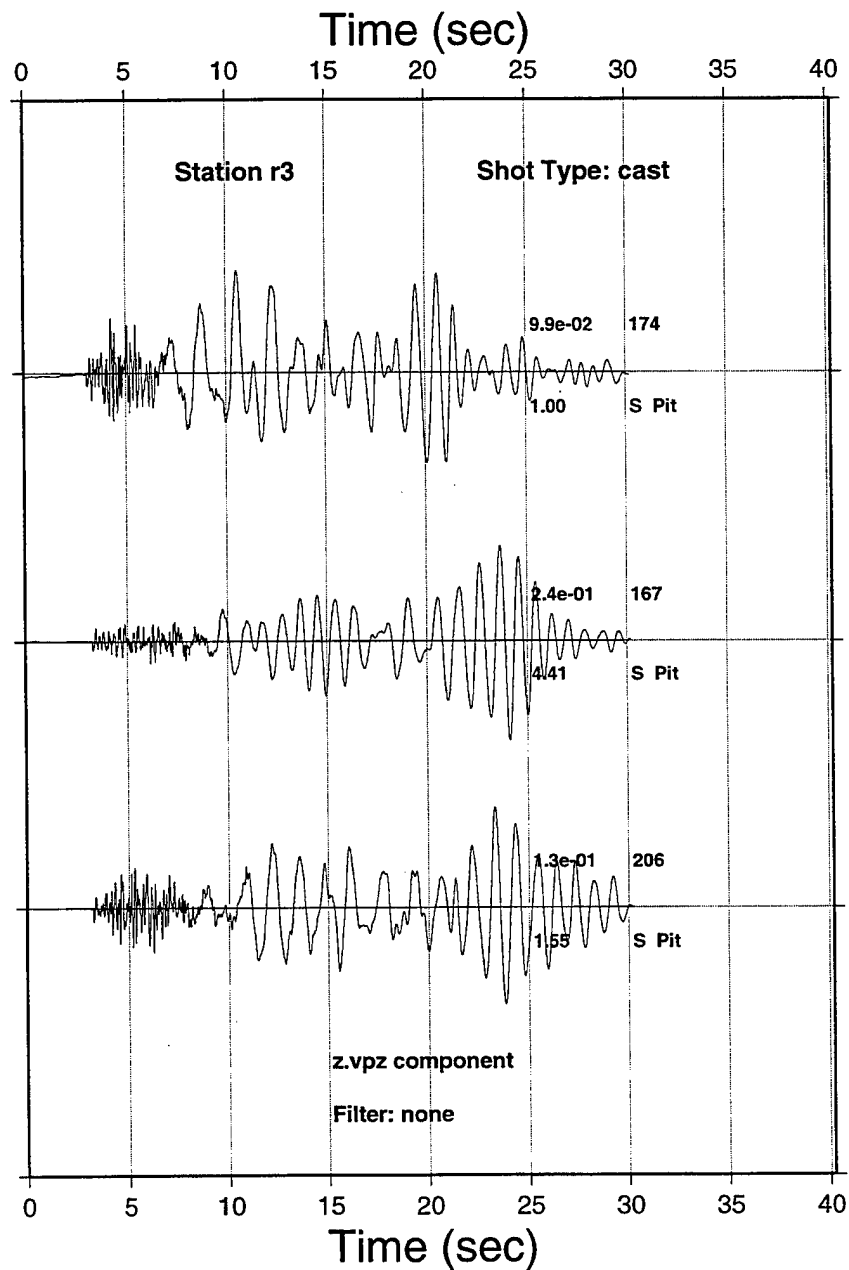


Figure 10. Vertical seismograms for three cast blasts in the south pit, recorded at R3.



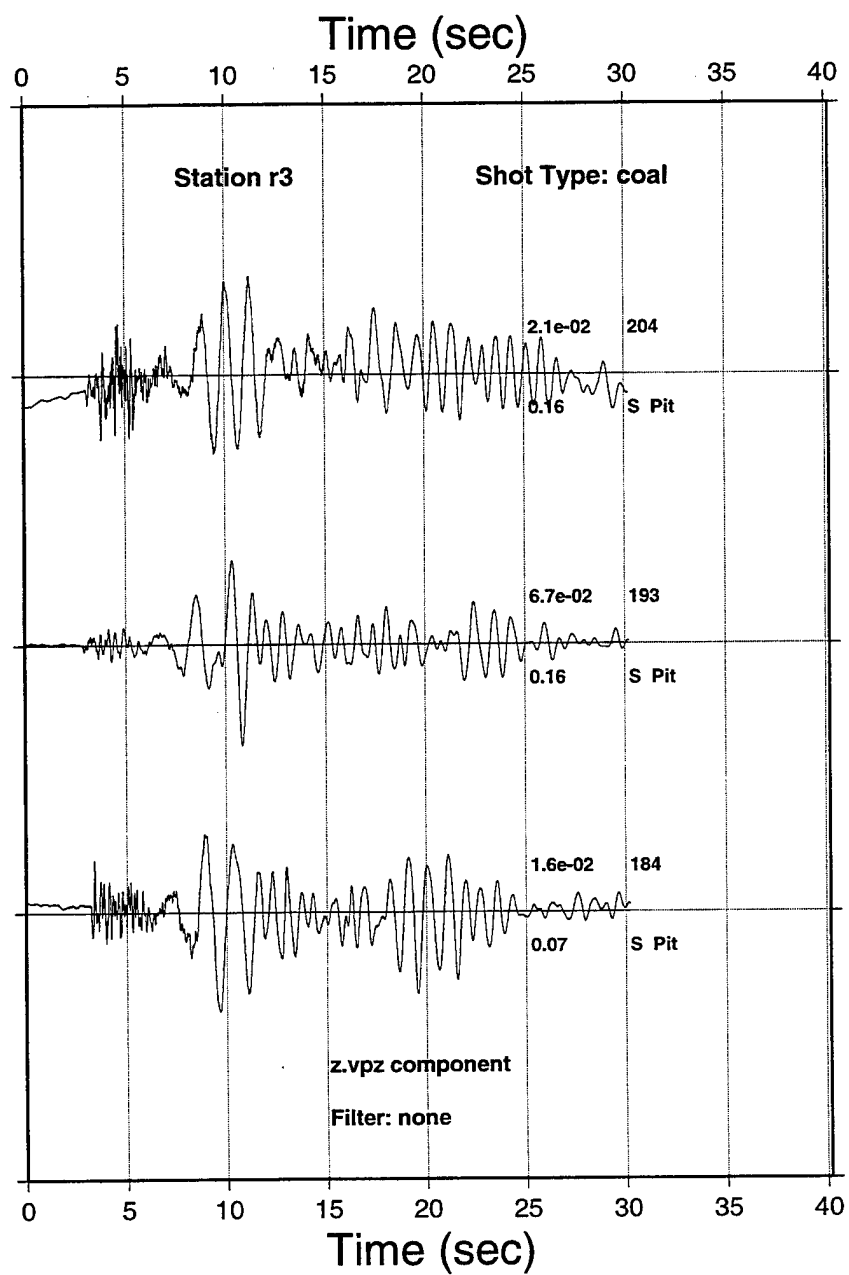


Figure 11. Vertical seismograms for three coal shots in the south pit, recorded at R3.

Visual inspection of the records from the different shot types indicates no apparent differences between the shot types. Recall that the early arriving, high frequency energy is associated with P waves and later, lower frequency energy is surface waves. We use as a measure of P and S energy the amplitudes of the early and late, respectively, signals. Figure 12 shows narrow band envelope functions of the vertical component for the cast shots at two center frequencies, 2 and 8 Hz. In each case, the bandwidth of the filter is 2 Hz. Also on the figure are S/P ratios computed from ratio of the peak S envelope at 2 Hz to the P envelope at 8 Hz. There is a factor of 5 variation in this parameter, with an average value of about 20.

Envelopes at 2 Hz (S)

Envelopes at 8 Hz (P)

S/P

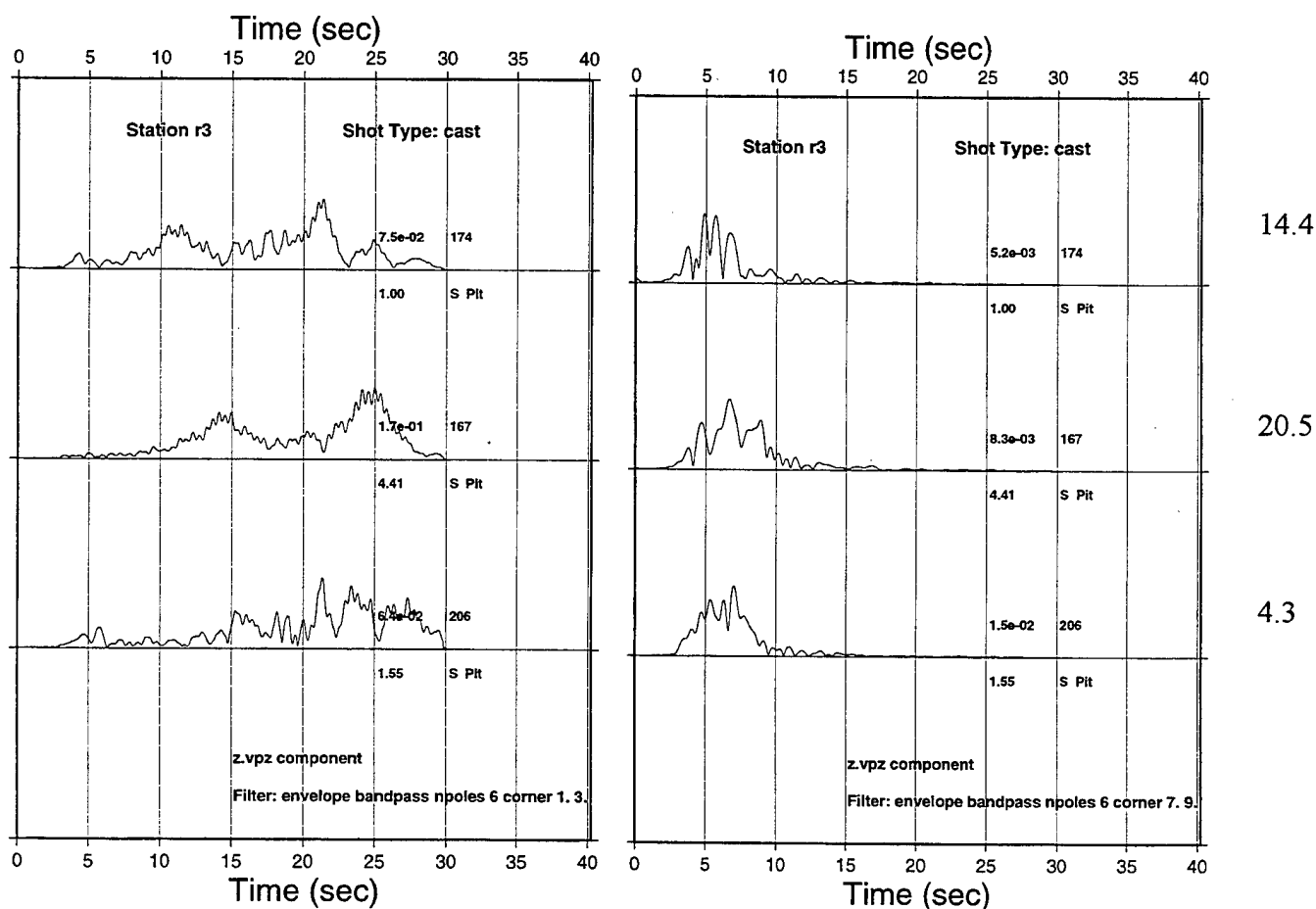


Figure 12. Narrow band envelope functions and S/P ratios (vertical component) for cast shots in the south pit at station R3.

A comparable plot for the coal shots is shown in Figure 13. The average S/P ratio is about 18, and the minimum and maximum values are similar to those from the cast blast. It appears that in the near field there are no significant differences in S/P excitation between the two source types. This comment applies to the radial and tangential components as well.

S/P

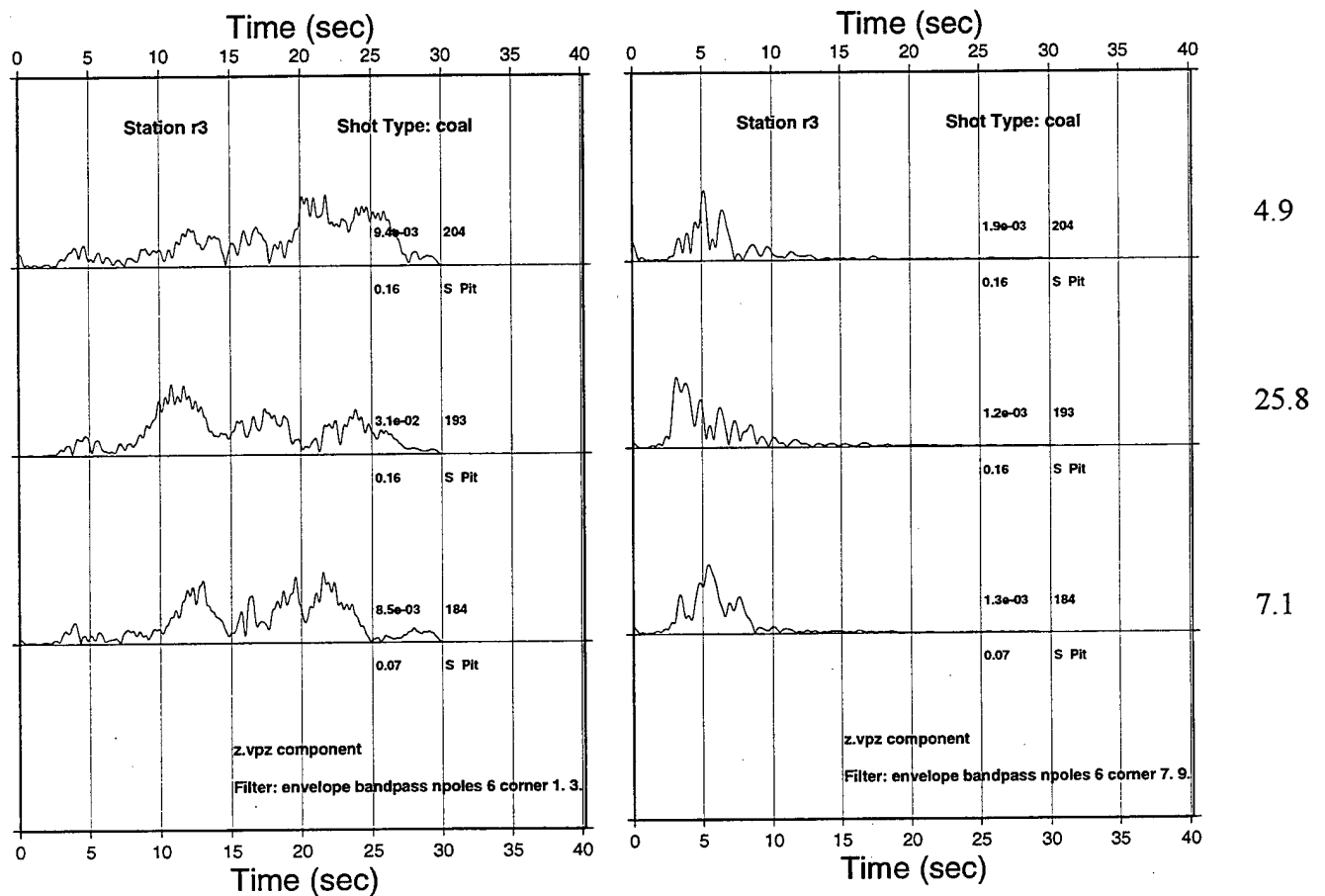


Figure 13. Narrow band envelope functions and S/P ratios (vertical component) for coal shots in the south pit at station R3.

In Figure 14, we compare three coal shots in the south pit and one in the west pit at station R3 (see Figure 1). The distance from the west pit shot to R3 (10.2 km) is slightly closer than the south pit shots (about 13 km), and the azimuth is closer to north. Recall that the west pit is aligned north-south while the south pit is aligned east-west. The differences between shots within the south pit are comparable to the differences between shots in the two pits.

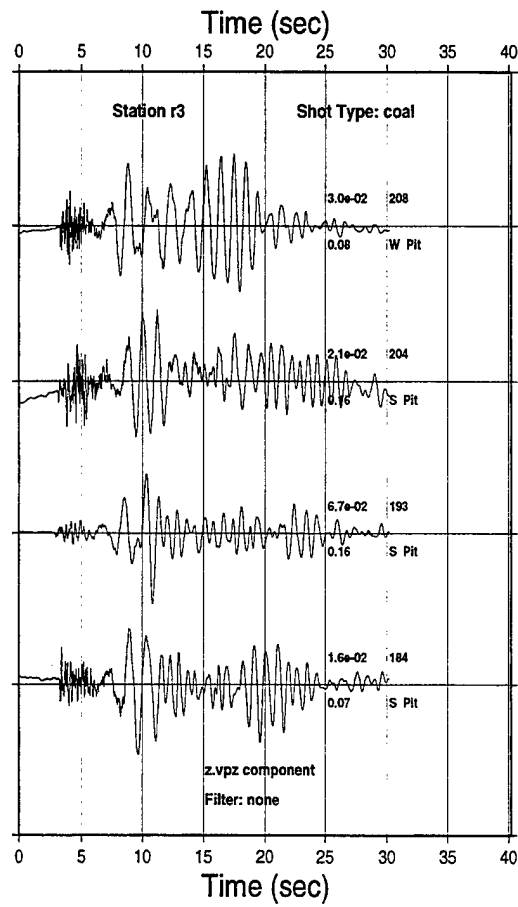


Figure 14. Vertical component seismograms from three coal shots in the south pit and one in the west pit at station R3.

In addition to S/P ratios, a feature often proposed as a discriminant is the spectral slope. In Table 3, we show spectral slopes of the surface waves for the shots in this data set. The slopes were computed by linear regression of the log of the amplitude spectrum versus log of frequency for frequencies above 1 Hz. The spectra are shown in Figure 15. The surface waves were chosen since their character is most likely to be indicative of Lg excitation. Three of the cast blasts have nearly the same slope, -1.6, but one shot (199) has a slope of -1.8. The coal shots have a greater scatter, ranging from -1 to -2.1, a range which brackets the cast blasts. The slope of the simultaneous coal shot lies in the ranges of both other shot types.

Table 3. Spectral slopes of the surface waves for the shots in this data set. The slopes were computed by linear regression of the log of the amplitude spectrum versus log of frequency for frequencies above 1 Hz

cast	
167	-1.59239
174	-1.55655
199	-1.83844
206	-1.57163
coal	
171	-1.71765
184	-1.62791
193	-2.10487
204	-1.20198
208	-0.975225
simultaneous	
236	-1.80378

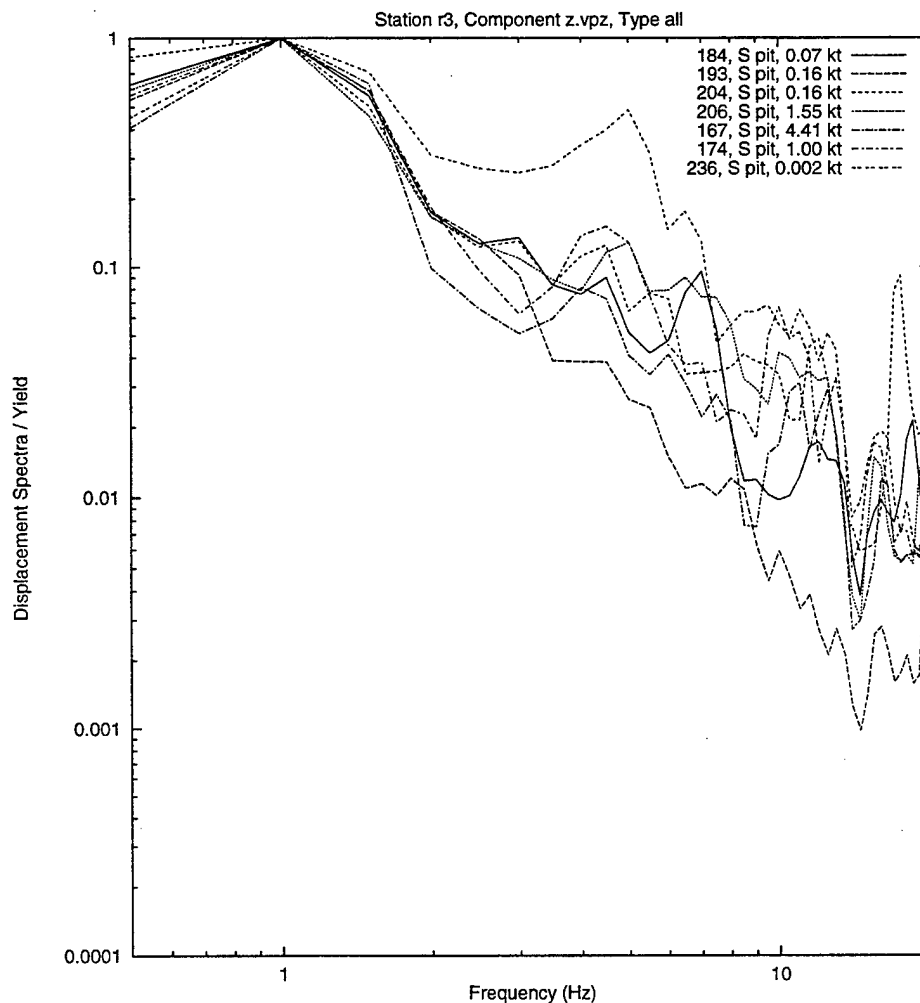


Figure 15. Spectral amplitudes of the surface waves for the shots recorded at station R3. Values have been normalized to the value at 1 Hz for each spectrum.

In summary, with regard to S/P ratios, spectral slopes and seismogram character, one cannot distinguish shot type or pit from these near-field data. In addition, we cannot determine whether this is characteristic of shots in the Black Thunder mine or whether this is characteristic of near-field data.

## 5.1 Inference of Source Structure, Comparison with Synthetics.

As mentioned above, signals at Black Thunder are strongly influenced by propagation effects. We have no independent information on earth structure or propagation properties, but we do have drilling reports. Thus, we adopted a strategy of using the source model proposed by Barker *et al.*, (1993a) with the parameters fixed by drilling reports and then varying propagation properties in order to match synthetic seismograms. This source model was used to interpret the Texas Chemline Quarry data in Bonner *et al.* (1996) and was the basis for the analyses of Black Thunder signals recorded at regional distances at PDAR by Anandakrishnan *et al.* (1997). The model consists of an explosive component and a spall or mass movement component. We focused on station R3, which is 11.6 km NNW of shot 236, the simultaneous coal shot (see Figure 1). This station was chosen since there are recordings there of several different source types and the range is great enough for seismic phases to separate in time.

Since only nominal shot times are available, structure could not be obtained from absolute travel times. As a first cut at identifying seismic phases, we made experiments using our surface wave modal program SYNSRF and earth structures appropriate to the geology (low velocity unconsolidated surficial sediments with a shallow coal seam). These calculations show that the signals which dominate the later parts of the records are fundamental and a few higher mode surface waves. We applied narrow-band filter analyses to the data to infer dispersion properties but interference between modes made interpretation unreliable. We had no formal inversion scheme that seemed applicable, so we opted for a parameter-space search of an earth model. We used the wavenumber integration code PROSE to compute propagation Green's functions which included body and surface waves for layered structures. Since it was found that the synthetic seismograms were sensitive to structure to a depth of about 200 m, we restricted our parameter search to those depths. The procedure was to vary the velocities in a model in which the upper 4 layers each had a thickness of 50 m, compute synthetic seismograms and compare the results to data. The shear velocities  $\beta$  of the layers were varied at 100 m/sec increments from 200 m/sec to 1000 m/sec, with the condition that the velocities increase with depth. The computed seismograms were most sensitive to  $\beta$  and  $Q_\beta$ , and relatively insensitive to compressional velocity  $\alpha$  and  $Q_\alpha$ , so the compressional values were set to be a multiple of the shear values. The procedure was repeated for several families of values of  $Q_\beta$ . In spite of the relative insensitivity to  $\alpha$ , it was possible to infer that the Poisson's ratio is high.

We began with the simultaneously detonated coal shot (236) since it should have had the most impulsive source function and least amount of mass movement relative to the cast blasts and the other (ripple-fired) coal shots. The simultaneously detonated coal shot is modeled as a grid of 5 rows (parallel to the shot face) by 3 columns of charges of equal yield for a total yield of 40,000 pounds. Charges are spaced at 10 m intervals. The purpose of a coal shot is to bulk the material and a significant amount of movement of the overburden is observed. Thus, a signal due to spall is added to a signal from the explosive detonation for each charge. The initial vertical velocity of the spalled material is assumed to be 3.5 m/sec. The tangential motion at station R3 is observed to be comparable to the

radial motion, so we further assume that the spall involves horizontal movement as well as vertical. The formulation for combining the spall and explosive time functions with the Green's functions is given by Barker *et al.* (1993b).

The Green's functions were convolved with the source functions and the results compared visually to the observations. The diagnostic features used to judge the goodness of fit were signal duration and relative timing and amplitude of apparent phases on the records. Particular attention was paid to the start and end times of the surface wave trains. The structure derived in this manner is shown in Figure 16. The structure in the surficial 100 m was verified by borehole measurements made recently in the vicinity (R. Nigbor, Agbabian Associates, personal communication).

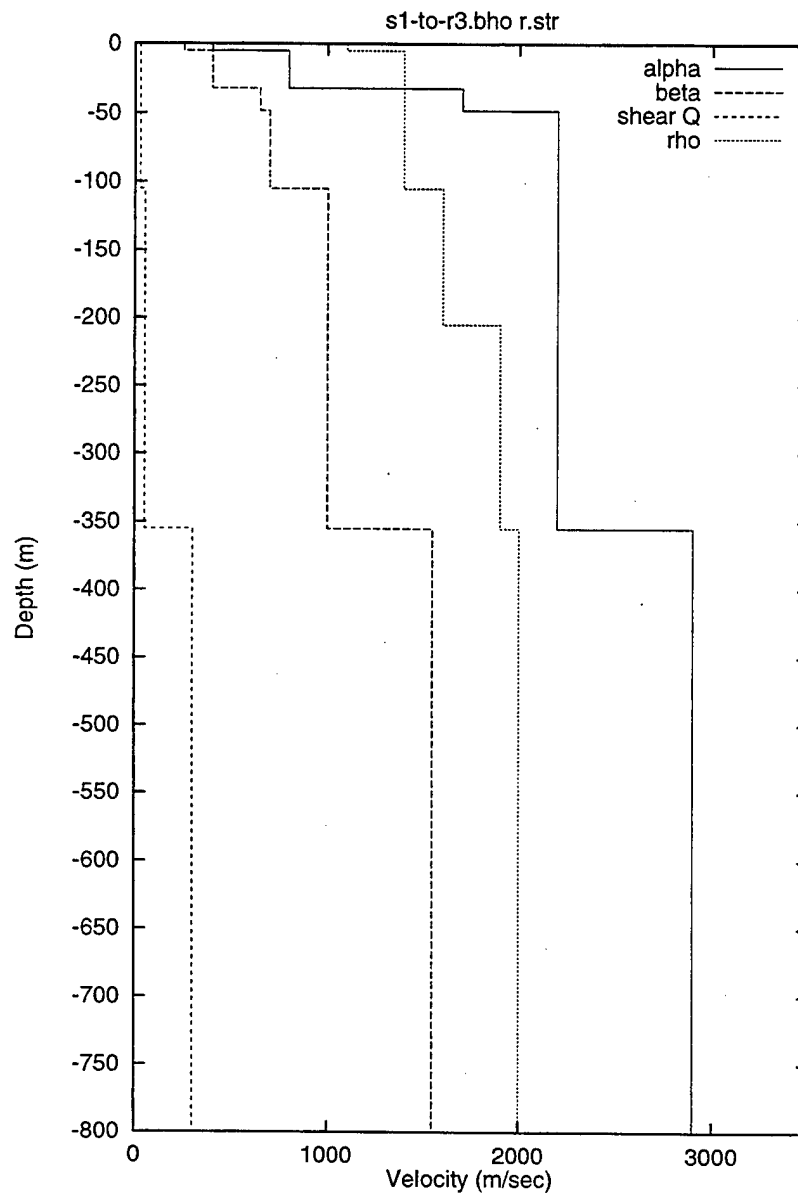


Figure 16. Earth structure used in the calculation of synthetic seismograms.



Figure 17 shows the explosive and spall or mass movement contributions to the synthetic vertical motion at R3 for the shot 174 source model. The peak motion, which is associated with the surface waves, from the explosive component is about 3 times the peak from the spall. The ratio of S to P motion due to the spall component exceeds 10 while the S/P ratio of the explosive part is about 3. The surface waves from the explosive component are largest late in the record (from 17 to 25 seconds), while those from the spall component arrive during the span from 10 to 25 seconds.

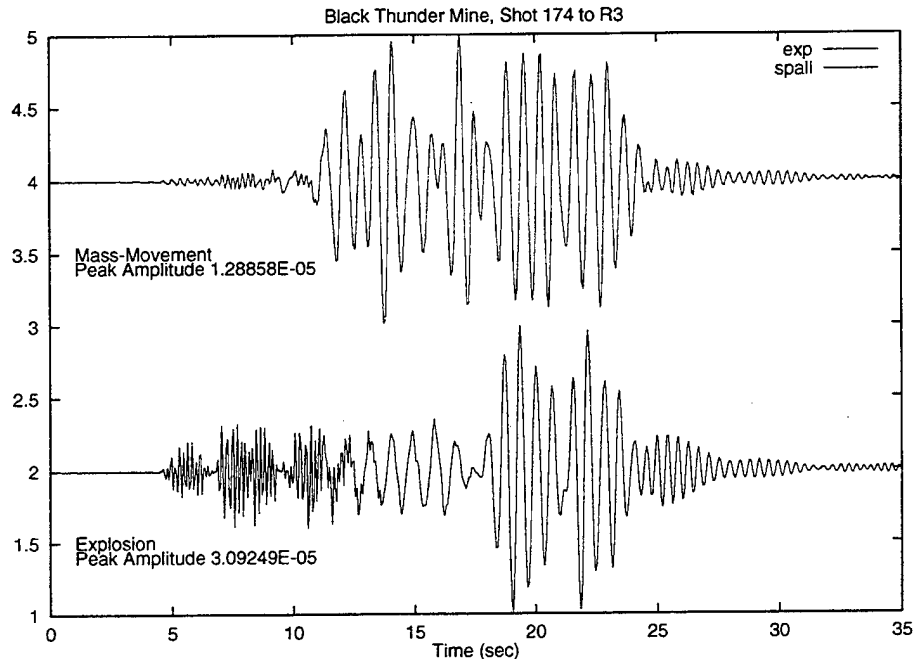


Figure 17. The spall and explosive contributions to the synthetic vertical motion at R3 for the shot 174 source model. The signals are globally scaled, with the peak motions indicated on the plot. The upper trace is the spall contribution and the lower trace is the explosive contribution.

Tangential synthetic and observed seismograms from coal shot 236 at R3 are compared in Figure 18. The data provided to us had been processed to remove the instrument response, which introduced a long period component, which detracted from this analysis. Thus, we have high pass filtered the time series at a corner frequency of 1 Hz to remove long period artifacts. The peak ground displacements from the synthetic record are within a factor of three of the observed record. The duration is matched fairly well, except for a small wave train after 25 sec. There is a phasing in the observed record that is roughly duplicated by the synthetic.

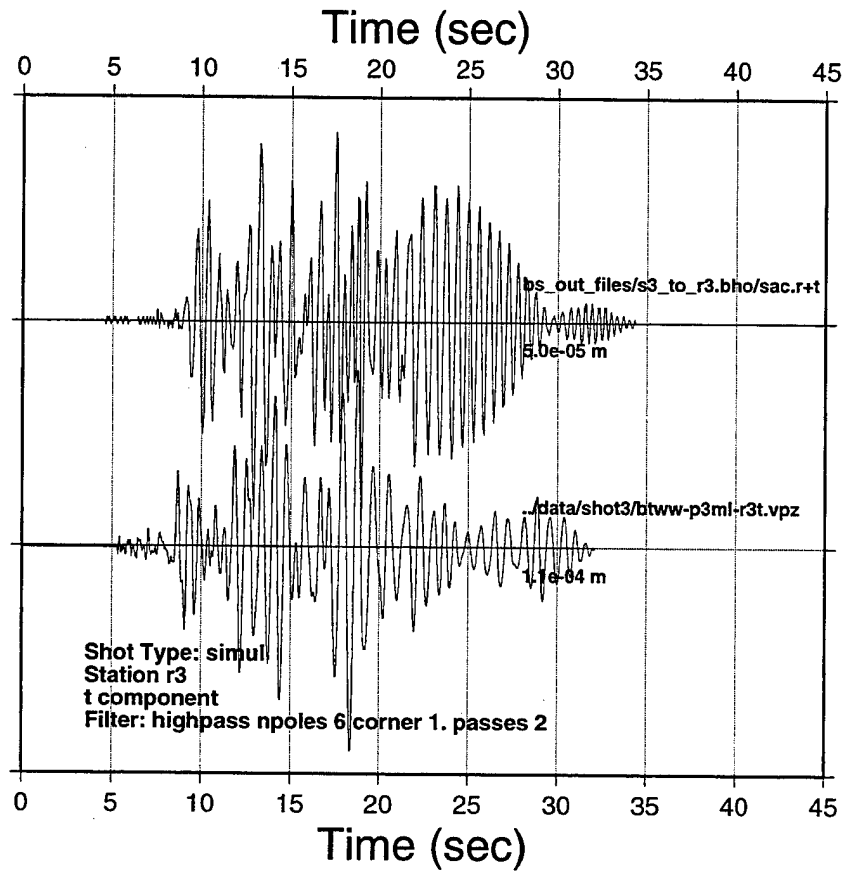


Figure 18. Tangential synthetic (upper) and observed (lower) displacement seismograms from coal shot 236 at R3. Peak displacements are indicated by the numbers below the time series (at the 30 sec line).

The corresponding vertical motions from the coal shot at R3 are shown in Figure 19. The synthetic vertical component seismograms include the explosive and vertical spall contributions. As with the tangential motions, the calculated peak displacement is about one third the observed value and the amplitude of the calculated signal arriving after 20 seconds is too small. To increase the amplitude of this late arriving energy, we tried increasing the values of  $Q$  in the surficial layers, but this did not produce the desired effect. We were unable to reproduce this late signal strength with reasonable values of seismic velocity in the shallow layers at this receiver location or at the closer station R2. Two explanations for this are (1) non-plane-layer propagation and (2) the actual source duration was longer than designed. A more complicated earth structure would not be expected to increase signal strength at both distances, so we hypothesize that the signal duration was longer than designed. The large high-frequency signal at the start of the observed record is probably caused by charges that did not fire according to the planned intervals. Because the calculated amplitudes are smaller than observed for both tangential and vertical components, we conclude that explosive coupling is higher than in the model and that there is significant conversion of P to S energy from the explosives. The mode conversion is consistent with calculations showing the effect of the quarry bench (Barker *et al.*, 1993b, McLaughlin *et al.*, 1994 and McLaughlin *et al.*, 1996).

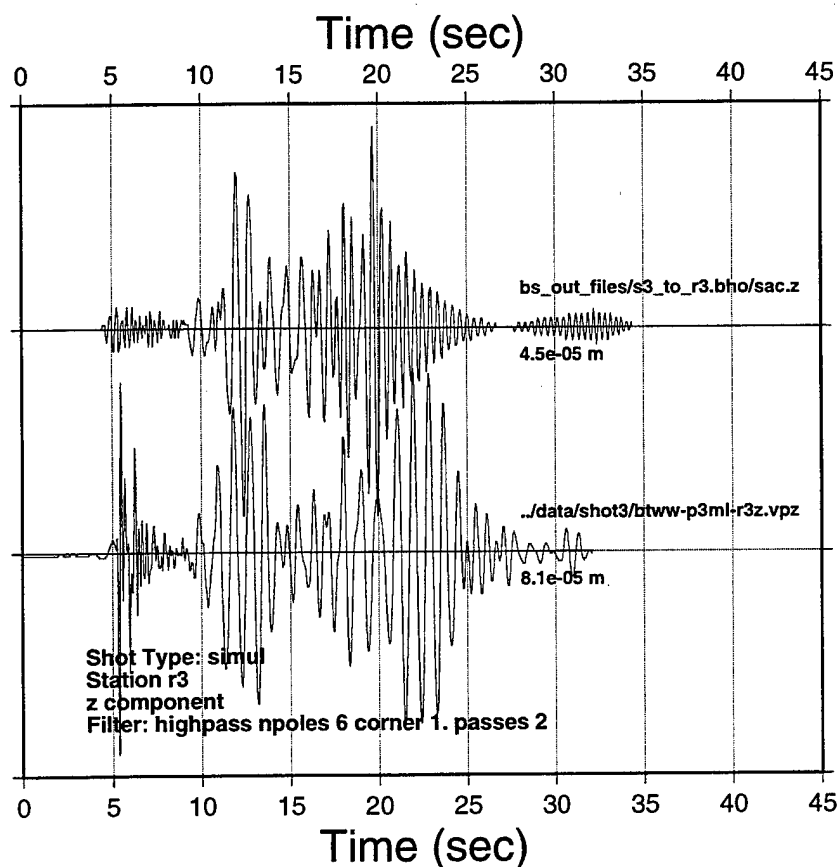


Figure 19. Vertical synthetic (upper) and observed (lower) displacement seismograms from coal shot 236 at R3. Peak displacements are indicated by the numbers below the time series (at the 30 sec line).

Additionally, the two large cast blasts were modeled. Cast blast 167 was modeled using 8 rows by 88 columns of charges, again at 10 m intervals. Time intervals followed the shot log design values which were that charges within columns were detonated at 35 ms intervals while rows were fired at times 125, 300, 500, 700, 900, 1200 and 1400 ms after the first row (Craig Pearson, LANL, personal communication). The initial velocity of the spalled material was assumed to be 3.5 m/sec with an initial angle of  $30^\circ$  from the horizontal. The shot was designed to throw material to the NE, which we assume to have occurred. Figure 20 shows tangential synthetic and observed seismograms from cast blast 167 at R3. The peak displacement is about one-fifth the observed value. The duration of the signals is longer than the coal shot 236, consistent with the increased duration of the blasting sequence. As with the coal shot, the relative amplitude of the late arriving signal (after 25 sec) is too small on the synthetic compared with the observed.

The vertical motions for cast blast 167 are shown in Figure 21. Again, the calculated peak amplitude and relative amplitude of late-arriving energy are less than observed. We conclude that we can achieve better agreement with observations by (1) increasing the source duration and (2) include P to S conversion from the explosive component of the source.

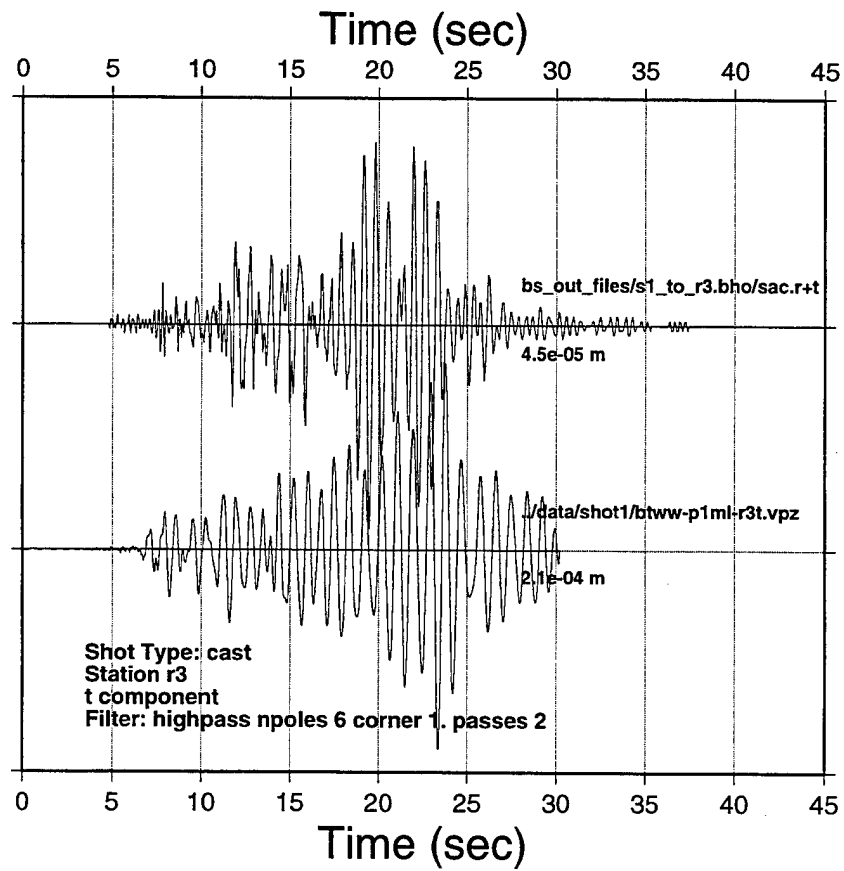


Figure 20. Tangential synthetic (upper) and observed (lower) displacement seismograms from cast blast 167 at R3. Peak displacements are indicated by the numbers below the time series (at the 30 sec line).

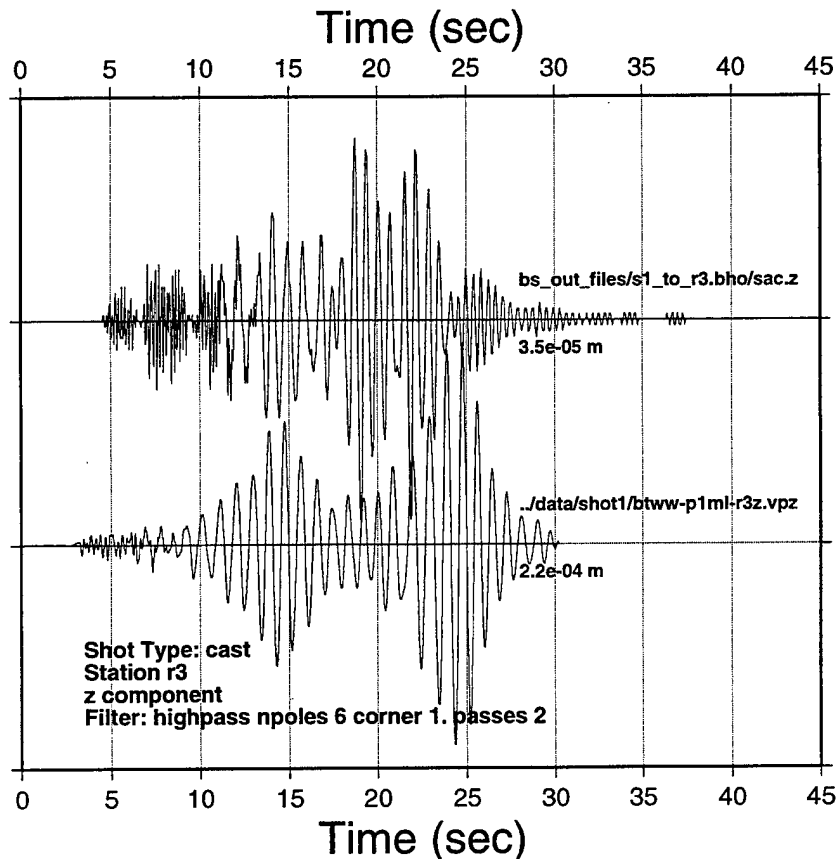


Figure 21. Vertical synthetic (upper) and observed (lower) displacement seismograms from cast blast 167 at R3. Peak displacements are indicated by the numbers below the time series (at the 30 sec line).

Consider next the other cast blast in this data set, shot 174. Recall that this shot was located near 167, but threw material to the NW. Cast blast 174 was modeled using 7 rows by 30 columns of charges with 10 m spacing. Time intervals followed the shot log design values which were that charges within columns were detonated at 35 ms intervals while rows were fired at times 125, 300, 500, 700, 900 and 1200 ms after the first row. Figures 22 and 23 show observed and synthetic tangential and vertical motions, respectively.

It is interesting to compare Figures 20 and 21 for shot 167 with Figures 22 and 23 for shot 174. Although the surface waves on the vertical components (Figures 20 and 22) are similar, the body waves from these shots show that signals from the same source type on the same face of the same pit can be quite different.

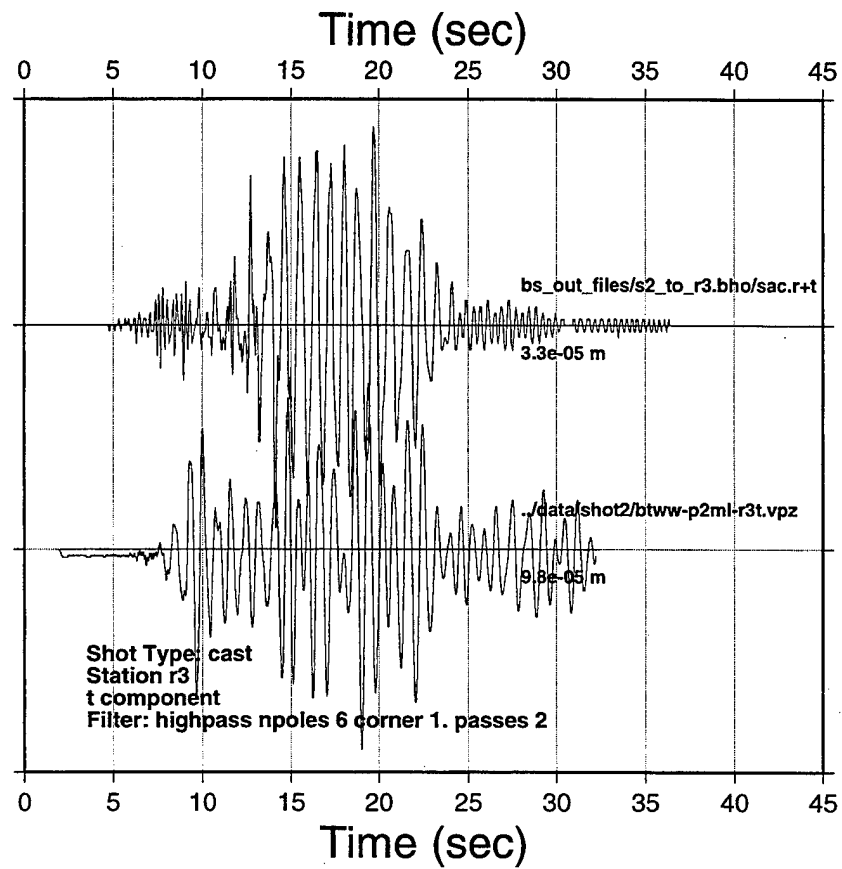


Figure 22. Tangential synthetic (upper) and observed (lower) displacement seismograms from cast blast 174 at R3. Peak displacements are indicated by the numbers below the time series (at the 30 sec line).

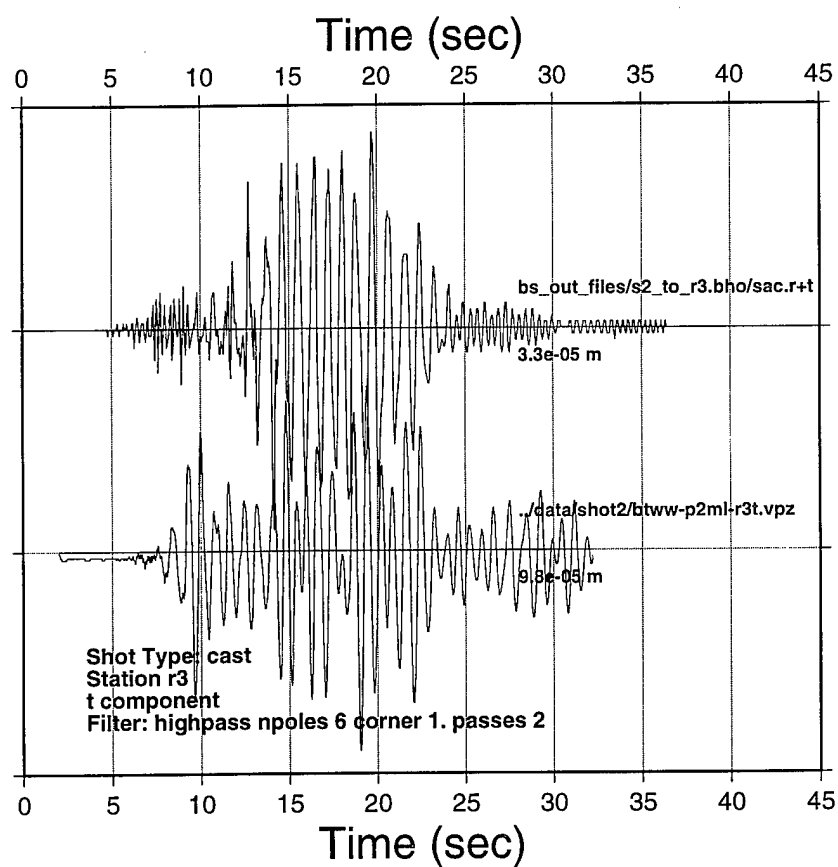


Figure 23. Vertical synthetic (upper) and observed (lower) displacement seismograms from cast blast 174 at R3. Peak displacements are indicated by the numbers below the time series (at the 30 sec line).

## 6.0 Black Thunder Mine Series: Regional Data

In addition to studies of the near-field data described above, we have begun analyses of near-regional data presented by Hedlin *et al.*, (1996). In the summer of 1996, IGPP/UCSD deployed five seismometers at ranges between 100 and 200 km from the Black Thunder mine, which augment the permanent regional stations RSSD and PDAR (Figure 24). Hedlin *et al.* (1996) recorded three large blasts, two in the South Pit (shots 214 and 215) and one in the North Pit (shot 201). During South Pit shot 215, a large fraction of the holes detonated simultaneously (unintentionally). Data from these shots were provided to us by Dr. Hedlin.

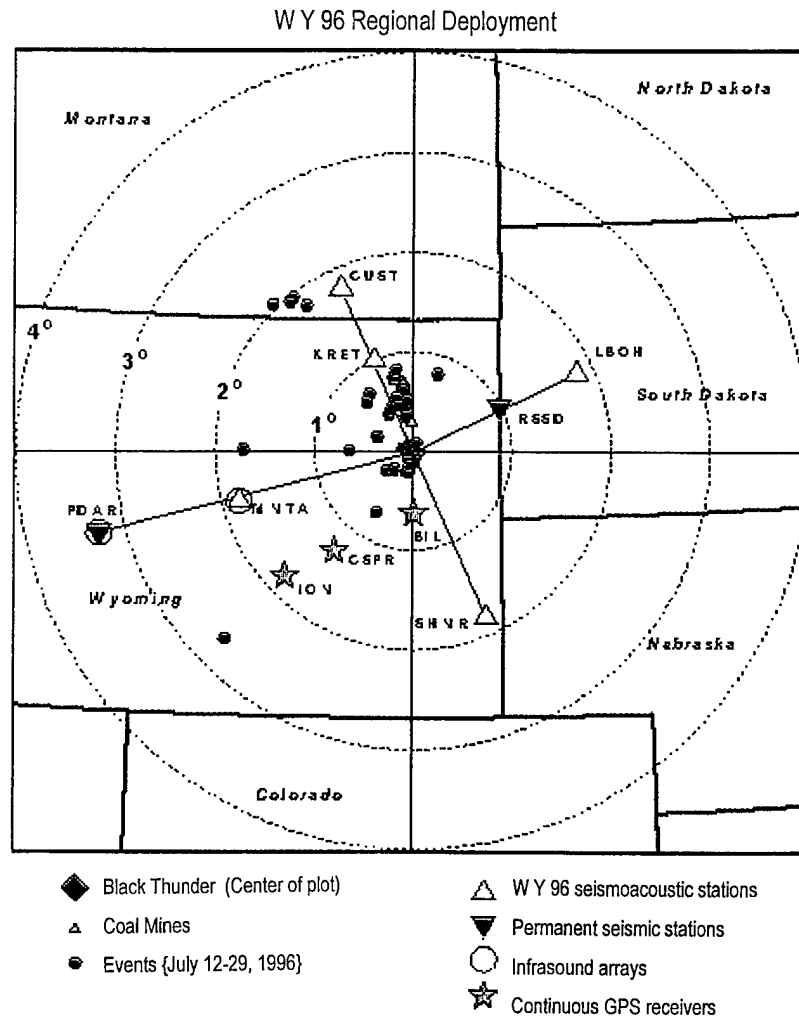


Figure 24. Map showing Black Thunder mine and stations deployed by Hedlin *et al.* (1996).



To isolate source properties, we inferred path properties to these sites. The signals have good Rayleigh waves, so we extracted dispersion curves and inverted them for earth structure using signals from three shots. Figure 25 shows the shear wave structures derived for each site using shot 201. The results are comparable for the other shots.

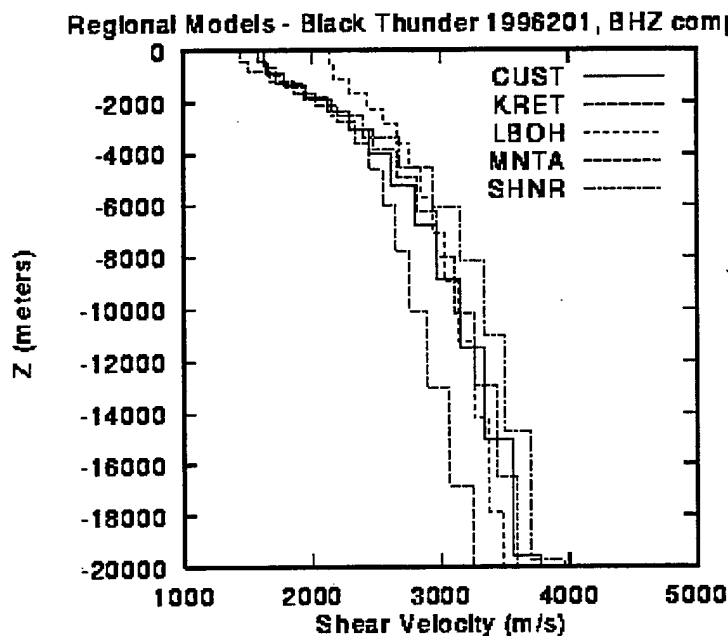
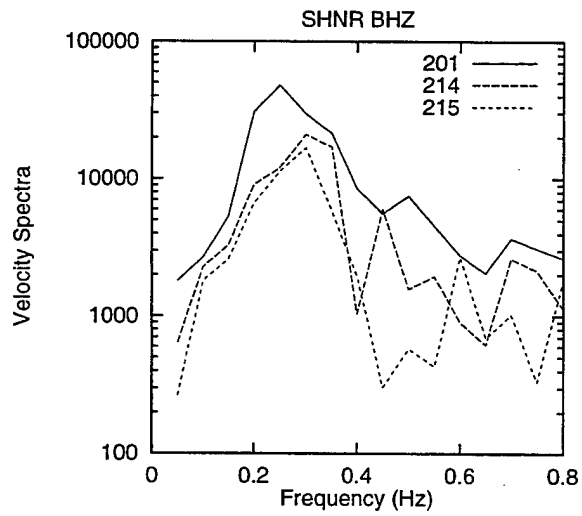
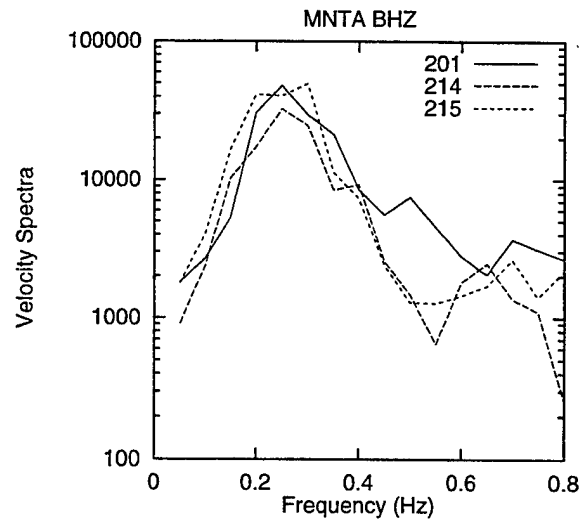


Figure 25. Shear velocity structure at four sites from the shot on Julian day 1996201.

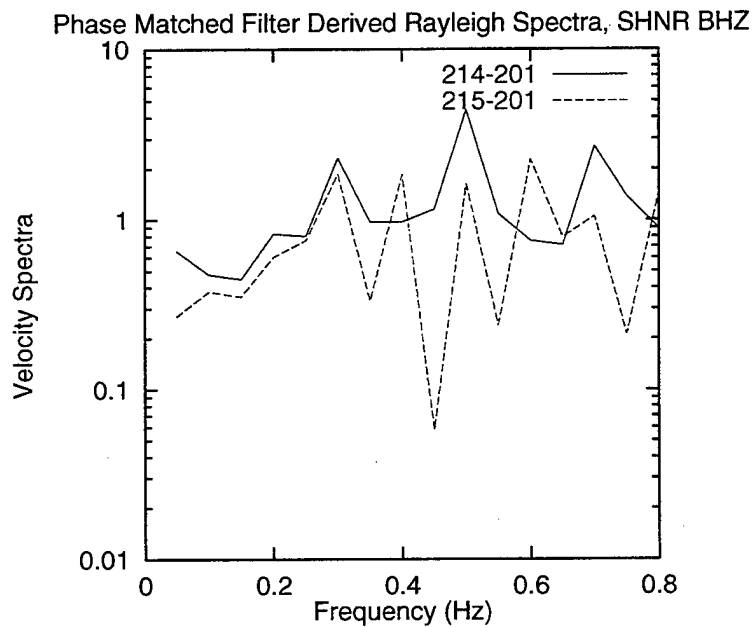
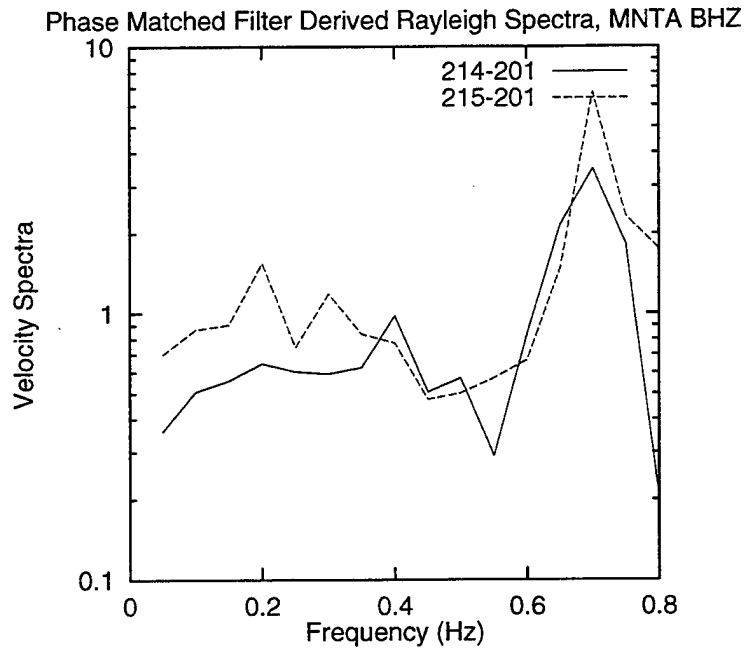
The models are quite consistent, with the exception of LBOH. These sites are all within the Powder River and Wind River Basins, except LBOH. Signals to LBOH are perhaps different because they must cross the Black Hills pluton.

Figures 26 a and b show spectra at stations MNTA and SHNR. The spectra have been corrected for propagation by using Rayleigh wave phase velocities as phase matched filters. At MNTA, the spectra from shots 214 and 215 (in the South Pit) are quite similar, while shot 201 (in the North Pit) is different from them. This would indicate that in this bandwidth the shot location (i.e., in which pit it occurs) influences the spectrum more than the firing pattern. This is the case at station SHNR below 0.4 Hz, but not as convincingly above 0.4 Hz.

To emphasize the South Pit spectra relative to the North Pit, the spectra for shots 214 and 215, divided by the corrected spectrum of shot 201, are shown in Figures 27 a and b for station MNTA and SHNR. Again, these figures indicate that source location has a stronger effect on amplitude than firing pattern at low frequencies.



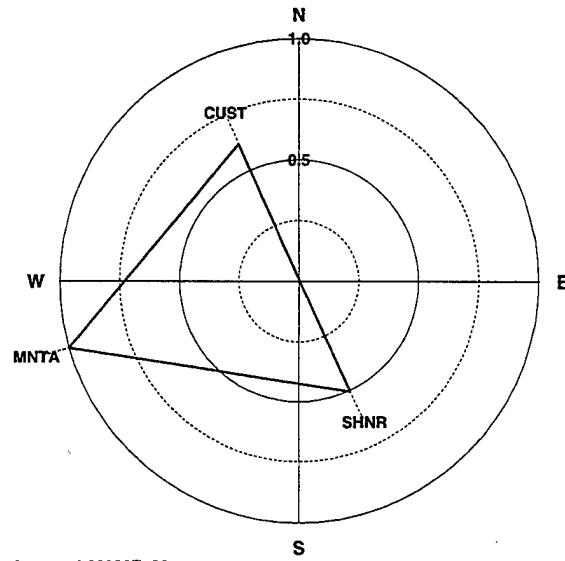
Figures 26 a and b. Log of spectra at stations MNTA (top) and SHNR (bottom). The spectra have been corrected for propagation by using Rayleigh wave phase velocities as phase matched filters.



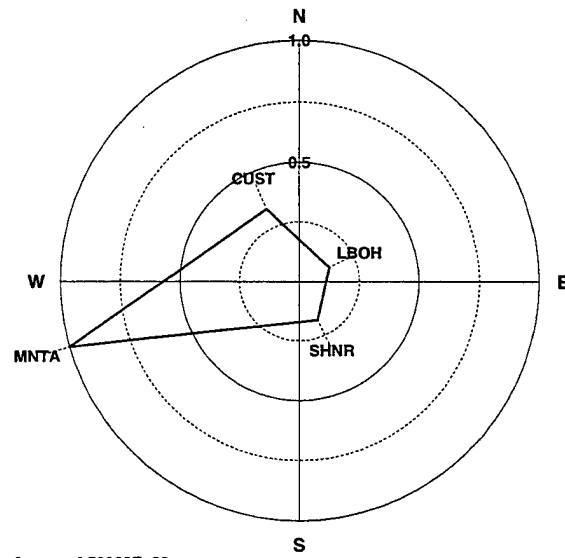
Figures 27 a and b. Log of spectra of South Pit shots 214 and 215 relative to North pit shot 201, at stations MNTA (top) and SHNR (bottom).

Radiation patterns of path corrected spectral amplitudes at 0.8 Hz for shots 201, 214 and 215 are shown in Figures 28, a to c. For this limited azimuthal coverage, it can be said that the radiation patterns for each shot are similar. For each shot, the peak motion is observed to the southwest at station MNTA, with intermediate values to the northwest and southeast. For this set of events at this frequency, shot location and firing pattern do not appear to affect Rayleigh wave radiation patterns. Bonner *et al.* (1996) observed variations in Rayleigh wave amplitudes in signals from a Texas quarry, but this was at higher frequencies (at which they could infer structure since their stations were much closer).

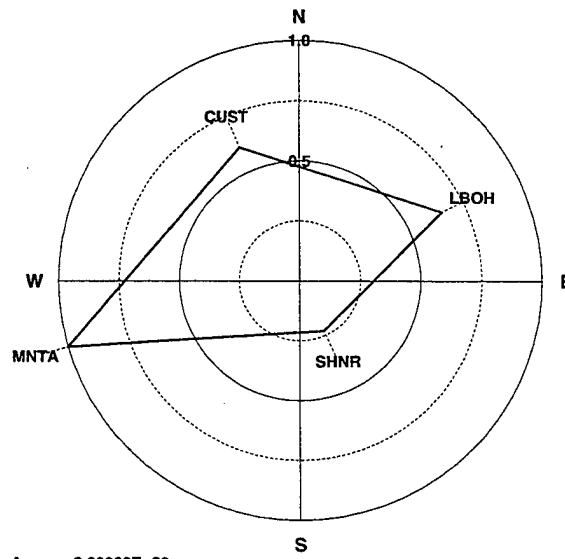
Shot 214



Amax = 1.60000E+23  
Shot 201



Amax = 4.50000E+23  
Shot 215



Amax = 2.30000E+23

Figure 28, a ,b,c. Radiation patterns of path corrected spectral amplitudes at 0.8 Hz for shots 201, 214 and 215.

## 7.0 Conclusions

We make the following conclusions.

1. Ripple firing effectively low pass filters the signals, in agreement with previous studies. Since for the near-field signals at Black Thunder, the observed high frequency components of the signals are associated with P waves and the lower frequency signals are associated with surface waves (dominated by shear motion), ripple firing has the indirect effect of increasing the S/P ratio in the seismograms.
2. We observe no consistent differences between motions from cast blasts and ripple-fired coal shots. In our previous numerical studies under this contract (Barker *et al.*, 1997) and in field studies (Bonner *et al.* 1996), azimuthal variations due to throw or strike of the bench were predicted and observed. We observe no differences between cast shots at the Black Thunder mine in which the throw or strike of the bench is different. We examined differences in seismogram character, S/P ratio and spectral slope. The lack of differences is due to the dominance of ground motion caused by explosions relative to that caused by mass movement, which is in turn is due to relative source coupling or propagation. Since differences in mass movement are the primary differences in the source mechanisms between coal and cast blasts, the dominance of the explosion component obscures the source mechanism.
3. Vertical and tangential near field ground motions (corrected for site response) from cast blasts are strongly enhanced normal to the bench in the direction of unmined land. We have no azimuthal coverage of a coal shot.
4. In contrast to the results of our previous studies in Texas (Barker *et al.*, 1997, Bonner *et al.* 1996), near-regional ground motions (corrected for path) show no azimuthal dependence on shot orientation.

## 8.0 References

- Anandakrishnan, S., S.R. Taylor and B.W. Stump, "Quantification and characterization of Regional Seismic Signals from Cast Blasting in Mines: a Linear Elastic Model," *Geophys. J. Intl.*, **131**(1), 45-60.
- Barker, T.G., K.L. McLaughlin and J.L. Stevens (1993a), "Numerical Simulation of Quarry Blast Sources," S-CUBED Technical Report to Phillips Laboratory, Kirtland AFB, SSS-TR-93-13859. ADA 265517
- Barker, T.G., K.L. McLaughlin, J.L. Stevens and S.M. Day (1993b), "Numerical Models of Quarry Blast Sources: the Effects of the Bench," S-CUBED Semiannual Report to Phillips Laboratory, Kirtland AFB, SSS-TR-93-13915. ADA 265370
- Barker, T.G., K.L. McLaughlin J.L. Stevens (1996), "Physical Mechanisms of Quarry Blast Sources," *Proceedings of the 18<sup>th</sup> Annual Seismic Research Symposium on Monitoring a Comprehensive Test Ban Treaty*, edited by J.F. Lewkowicz, J.M. McPhetres and D.T. Reiter, Annapolis MD, PL-TR-96-2153, ADA313692.
- Barker, T.G., K.L. McLaughlin, J. L. Bonner (1997), "Physical Mechanisms of Quarry Blast Sources," Maxwell Technologies Scientific Report to Department of Energy and Phillips Laboratory, MFD-TR-97-15695.
- Bonner, J.L. and T. Goforth (1995), "Characteristics of Rg Waves Recorded from Quarry Blasts," *Bull. Seism. Soc. Am.*, **85**, pp. 1232-1235.
- Bonner, J.L., E. Herrin and T. Goforth (1996), "Azimuthal Variation of Rg Energy in Central Texas," *Geophys. Res. Lett.*, **67**, (4), pp. 43-56.
- Day, S.M. and K.L. McLaughlin (1991), "Seismic Source Representations for Spall," *Bull. Seism. Soc. Am.*, **81**, pp. 191-201.
- Delitsyne, L. (1996), "Generation of Shear Waves from Quarries from Near-Regional Data," *Seism. Res. Lett.*, **67**, (2), p. 36.
- Hedlin, M.A.H., F.L. Vernon, J.B. Minster and J.A. Orcutt (1996), "Experiments in Regional Monitoring of Small Seismic/Acoustic Events," *Proceedings of the 18<sup>th</sup> Annual Seismic Research Symposium on Monitoring a Comprehensive Test Ban Treaty*, edited by J.F. Lewkowicz, J.M. McPhetres and D.T. Reiter, Annapolis MD, PL-TR-96-2153, ADA313692.
- Konya and Walter (1990), *Surface Blast Design*, Prentice Hall, 303 pages.

- McLaughlin, K.L., T.G. Barker and J.L. Stevens (1994), "Numerical Simulation of Quarry Blast Sources," S-CUBED Final Report to Phillips Laboratory, Kirtland AFB, SSS-TR-94-14418. ADA275799
- McLaughlin, K. L., J. Bonner and T. G. Barker (1996), "Seismic Source Mechanisms for Quarry Blasts Observed Rayleigh and Love Wave Radiation Patterns from a Texas Quarry," in preparation.
- Stump, B.W. and R.E. Reinke (1988), "Experimental Confirmation of Superposition from Small-Scale Explosions," *Bull. Seism. Soc. Am.*, **78**, pp. 1059-1073
- Stump, B.W., D.C. Pearson, R.L. Martin, P.E. Harben, C.L. Edwards, D. Baker, K. Kihara, K. Dalrymple, J.P. Lewis, D. Rock and R. Boyd, "The Black Thunder Regional Seismic Experiment," LANL Report LAUL-95-3980.
- Taylor, S.R. and G.E. Randall (1989), "The Effects of Spall on Regional Seismograms," *Geophys. Res. Lett.*, **16**, 211-214.

THOMAS AHRENS  
SEISMOLOGICAL LABORATORY 252-21  
CALIFORNIA INST. OF TECHNOLOGY  
PASADENA, CA 91125

AIR FORCE RESEARCH LABORATORY  
ATTN: VSOE  
29 RANDOLPH ROAD  
HANSCom AFB, MA 01731-3010 (2 COPIES)

AIR FORCE RESEARCH LABORATORY  
ATTN: RESEARCH LIBRARY/TL  
5 WRIGHT STREET  
HANSCom AFB, MA 01731-3004

AIR FORCE RESEARCH LABORATORY  
ATTN: AFRL/SUL  
3550 ABERDEEN AVE SE  
KIRTLAND AFB, NM 87117-5776 (2 COPIES)

RALPH ALEWINE  
NTPO  
1901 N. MOORE STREET, SUITE 609  
ARLINGTON, VA 22209

MUAWIA BARAZANGI  
INSTOC  
3126 SNEE HALL  
CORNELL UNIVERSITY  
ITHACA, NY 14853

T.G. BARKER  
MAXWELL TECHNOLOGIES  
8888 BALBOA AVE.  
SAN DIEGO, CA 92123-1506

DOUGLAS BAUMGARDT  
ENSCO INC.  
5400 PORT ROYAL ROAD  
SPRINGFIELD, VA 22151

THERON J. BENNETT  
MAXWELL TECHNOLOGIES  
11800 SUNRISE VALLEY  
SUITE 1212  
RESTON, VA 22091

WILLIAM BENSON  
NAS/COS  
ROOM HA372  
2001 WISCONSIN AVE. NW  
WASHINGTON DC 20007

JONATHAN BERGER  
UNIV. OF CALIFORNIA, SAN DIEGO  
SCRIPPS INST. OF OCEANOGRAPHY IGPP, 0225  
9500 GILMAN DRIVE  
LA JOLLA, CA 92093-0225

ROBERT BLANDFORD  
AFTAC  
1300 N. 17TH STREET  
SUITE 1450  
ARLINGTON, VA 22209-2308

LESLIE A. CASEY  
DEPT. OF ENERGY/NN-20  
1000 INDEPENDENCE AVE. SW  
WASHINGTON DC 20585-0420

CENTER FOR MONITORING RESEARCH  
ATTN: LIBRARIAN  
1300 N. 17th STREET, SUITE 1450  
ARLINGTON, VA 22209

ANTON DAINTY  
HQ DSWA/PMA  
6801 TELEGRAPH ROAD  
ALEXANDRIA, VA 22310-3398

CATHERINE DE GROOT-HEDLIN  
UNIV. OF CALIFORNIA, SAN DIEGO  
IGPP  
8604 LA JOLLA SHORES DRIVE  
SAN DIEGO, CA 92093

DIANE DOSER  
DEPT. OF GEOLOGICAL SCIENCES  
THE UNIVERSITY OF TEXAS AT EL PASO  
EL PASO, TX 79968

DTIC  
8725 JOHN J. KINGMAN ROAD  
FT BELVOIR, VA 22060-6218 (2 COPIES)

MARK D. FISK  
MISSION RESEARCH CORPORATION  
735 STATE STREET  
P.O. DRAWER 719  
SANTA BARBARA, CA 93102-0719

LORI GRANT  
MULTIMAX, INC.  
311C FOREST AVE. SUITE 3  
PACIFIC GROVE, CA 93950



HENRY GRAY  
SMU STATISTICS DEPARTMENT  
P.O. BOX 750302  
DALLAS, TX 75275-0302

DAVID HARKRIDER  
BOSTON COLLEGE  
INSTITUTE FOR SPACE RESEARCH  
140 COMMONWEALTH AVENUE  
CHESTNUT HILL, MA 02167

MICHAEL HEDLIN  
UNIVERSITY OF CALIFORNIA, SAN DIEGO  
SCRIPPS INST. OF OCEANOGRAPHY  
9500 GILMAN DRIVE  
LA JOLLA, CA 92093-0225

EUGENE HERRIN  
SOUTHERN METHODIST UNIVERSITY  
DEPT. OF GEOLOGICAL SCIENCES  
DALLAS, TX 75275-0395

VINDELL HSU  
HQ/AFTAC/TTR  
1030 S. HIGHWAY A1A  
PATRICK AFB, FL 32925-3002

THOMAS JORDAN  
MASS. INST. OF TECHNOLOGY  
BLDG 54-918  
CAMBRIDGE, MA 02139

LAWRENCE LIVERMORE NAT'L LAB  
ATTN: TECHNICAL STAFF (PLS ROUTE)  
PO BOX 808, MS L-208  
LIVERMORE, CA 94551

LAWRENCE LIVERMORE NAT'L LAB  
ATTN: TECHNICAL STAFF (PLS ROUTE)  
PO BOX 808, MS L-200  
LIVERMORE, CA 94551

THORNE LAY  
UNIV. OF CALIFORNIA, SANTA CRUZ  
EARTH SCIENCES DEPARTMENT  
EARTH & MARINE SCIENCE BUILDING  
SANTA CRUZ, CA 95064

I. N. GUPTA  
MULTIMAX, INC.  
1441 MCCORMICK DRIVE  
LARGO, MD 20774

THOMAS HEARN  
NEW MEXICO STATE UNIVERSITY  
DEPARTMENT OF PHYSICS  
LAS CRUCES, NM 88003

DONALD HELMBERGER  
CALIFORNIA INST. OF TECHNOLOGY  
DIV. OF GEOL. & PLANETARY SCIENCES  
SEISMOLOGICAL LABORATORY  
PASADENA, CA 91125

ROBERT HERRMANN  
ST. LOUIS UNIVERSITY  
DEPT. OF EARTH & ATMOS. SCIENCES  
3507 LACLEDE AVENUE  
ST. LOUIS, MO 63103

RONG-SONG JIH  
HQ DSWA/PMA  
6801 TELEGRAPH ROAD  
ALEXANDRIA, VA 22310-3398

LAWRENCE LIVERMORE NAT'L LAB  
ATTN: TECHNICAL STAFF (PLS ROUTE)  
PO BOX 808, MS L-175  
LIVERMORE, CA 94551

LAWRENCE LIVERMORE NAT'L LAB  
ATTN: TECHNICAL STAFF (PLS ROUTE)  
PO BOX 808, MS L-202  
LIVERMORE, CA 94551

LAWRENCE LIVERMORE NAT'L LAB  
ATTN: TECHNICAL STAFF (PLS ROUTE)  
PO BOX 808, MS L-205  
LIVERMORE, CA 94551

LAWRENCE LIVERMORE NAT'L LAB  
ATTN: TECHNICAL STAFF (PLS ROUTE)  
PO BOX 808, MS L-221  
LIVERMORE, CA 94551

ANATOLI L. LEVSHIN  
DEPARTMENT OF PHYSICS  
UNIVERSITY OF COLORADO  
CAMPUS BOX 390  
BOULDER, CO 80309-0309

JAMES LEWKOWICZ  
WESTON GEOPHYSICAL CORP.  
325 WEST MAIN STREET  
NORTHBORO, MA 01532

LOS ALAMOS NATIONAL LABORATORY  
ATTN: TECHNICAL STAFF (PLS ROUTE)  
PO BOX 1663, MS F659  
LOS ALAMOS, NM 87545

LOS ALAMOS NATIONAL LABORATORY  
ATTN: TECHNICAL STAFF (PLS ROUTE)  
PO BOX 1663, MS F665  
LOS ALAMOS, NM 87545

LOS ALAMOS NATIONAL LABORATORY  
ATTN: TECHNICAL STAFF (PLS ROUTE)  
PO BOX 1663, MS C335  
LOS ALAMOS, NM 87545

GARY MCCARTOR  
SOUTHERN METHODIST UNIVERSITY  
DEPARTMENT OF PHYSICS  
DALLAS, TX 75275-0395

KEITH MCLAUGHLIN  
CENTER FOR MONITORING RESEARCH  
SAIC  
1300 N. 17TH STREET, SUITE 1450  
ARLINGTON, VA 22209

BRIAN MITCHELL  
DEPARTMENT OF EARTH & ATMOSPHERIC SCIENCES  
ST. LOUIS UNIVERSITY  
3507 LACLEDE AVENUE  
ST. LOUIS, MO 63103

RICHARD MORROW  
USACDA/IVI  
320 21ST STREET, N.W.  
WASHINGTON DC 20451

JOHN MURPHY  
MAXWELL TECHNOLOGIES  
11800 SUNRISE VALLEY DRIVE  
SUITE 1212  
RESTON, VA 22091

JAMES NI  
NEW MEXICO STATE UNIVERSITY  
DEPARTMENT OF PHYSICS  
LAS CRUCES, NM 88003

ROBERT NORTH  
CENTER FOR MONITORING RESEARCH  
1300 N. 17th STREET, SUITE 1450  
ARLINGTON, VA 22209

OFFICE OF THE SECRETARY OF DEFENSE  
DDR&E  
WASHINGTON DC 20330

JOHN ORCUTT  
INST. OF GEOPH. & PLANETARY PHYSICS  
UNIV. OF CALIFORNIA, SAN DIEGO  
LA JOLLA, CA 92093

PACIFIC NORTHWEST NAT'L LAB  
ATTN: TECHNICAL STAFF (PLS ROUTE)  
PO BOX 999, MS K6-48  
RICHLAND, WA 99352

PACIFIC NORTHWEST NAT'L LAB  
ATTN: TECHNICAL STAFF (PLS ROUTE)  
PO BOX 999, MS K6-40  
RICHLAND, WA 99352

PACIFIC NORTHWEST NAT'L LAB  
ATTN: TECHNICAL STAFF (PLS ROUTE)  
PO BOX 999, MS K6-84  
RICHLAND, WA 99352

PACIFIC NORTHWEST NAT'L LAB  
ATTN: TECHNICAL STAFF (PLS ROUTE)  
PO BOX 999, MS K5-12  
RICHLAND, WA 99352

FRANK PILOTTE  
HQ AFTAC/TT  
1030 S. HIGHWAY A1A  
PATRICK AFB, FL 32925-3002

KEITH PRIESTLEY  
DEPARTMENT OF EARTH SCIENCES  
UNIVERSITY OF CAMBRIDGE  
MADINGLEY RISE, MADINGLEY ROAD  
CAMBRIDGE, CB3 0EZ UK

JAY PULLI  
BBN SYSTEMS AND TECHNOLOGIES, INC.  
1300 NORTH 17TH STREET  
ROSSLYN, VA 22209

DELAINE REITER  
AFRL/VSOE (SENCOM)  
73 STANDISH ROAD  
WATERTOWN, MA 02172

PAUL RICHARDS  
COLUMBIA UNIVERSITY  
LAMONT-DOHERTY EARTH OBSERV.  
PALISADES, NY 10964

MICHAEL RITZWOLLER  
DEPARTMENT OF PHYSICS  
UNIVERSITY OF COLORADO  
CAMPUS BOX 390  
BOULDER, CO 80309-0309

DAVID RUSSELL  
HQ AFTAC/TTR  
1030 SOUTH HIGHWAY A1A  
PATRICK AFB, FL 32925-3002

\* CHANDAN SAIKIA  
WOODWARD-CLYDE FED. SERVICES  
566 EL DORADO ST., SUITE 100  
\* PASADENA, CA 91101-2560

SANDIA NATIONAL LABORATORY  
ATTN: TECHNICAL STAFF (PLS ROUTE)  
DEPT. 5704  
MS 0979, PO BOX 5800  
ALBUQUERQUE, NM 87185-0979

SANDIA NATIONAL LABORATORY  
ATTN: TECHNICAL STAFF (PLS ROUTE)  
DEPT. 9311  
MS 1159, PO BOX 5800  
ALBUQUERQUE, NM 87185-1159

SANDIA NATIONAL LABORATORY  
ATTN: TECHNICAL STAFF (PLS ROUTE)  
DEPT. 5704  
MS 0655, PO BOX 5800  
ALBUQUERQUE, NM 87185-0655

SANDIA NATIONAL LABORATORY  
ATTN: TECHNICAL STAFF (PLS ROUTE)  
DEPT. 5736  
MS 0655, PO BOX 5800  
ALBUQUERQUE, NM 87185-0655

THOMAS SERENO JR.  
SAIC  
10260 CAMPUS POINT DRIVE  
SAN DIEGO, CA 92121

AVI SHAPIRA  
SEISMOLOGY DIVISION  
IPRG  
P.O.B. 2286 NOLON 58122 ISRAEL

ROBERT SHUMWAY  
410 MRAK HALL  
DIVISION OF STATISTICS  
UNIVERSITY OF CALIFORNIA  
DAVIS, CA 95616-8671

MATTHEW SIBOL  
ENSCO, INC.  
445 PINEDA CT.  
MELBOURNE, FL 32940

DAVID SIMPSON  
IRIS  
1200 NEW YORK AVE., NW  
SUITE 800  
WASHINGTON DC 20005

JEFFRY STEVENS  
MAXWELL TECHNOLOGIES  
8888 BALBOA AVE.  
\* SAN DIEGO, CA 92123-1506

BRIAN SULLIVAN  
BOSTON COLLEGE  
INSITUTE FOR SPACE RESEARCH  
140 COMMONWEALTH AVENUE  
CHESTNUT HILL, MA 02167

\* TACTEC  
BATTELLE MEMORIAL INSTITUTE  
505 KING AVENUE  
COLUMBUS, OH 43201 (FINAL REPORT)

NAFI TOKSOZ  
EARTH RESOURCES LABORATORY  
M.I.T.  
42 CARLTON STREET, E34-440  
CAMBRIDGE, MA 02142

LAWRENCE TURNBULL  
ACIS  
DCI/ACIS  
WASHINGTON DC 20505

GREG VAN DER VINK  
IRIS  
1200 NEW YORK AVE., NW  
SUITE 800  
WASHINGTON DC 20005

FRANK VERNON  
UNIV. OF CALIFORNIA, SAN DIEGO  
SCRIPPS INST. OF OCEANOGRAPHY  
9500 GILMAN DRIVE  
LA JOLLA, CA 92093-0225

JILL WARREN  
LOS ALAMOS NATIONAL LABORATORY  
GROUP NIS-8  
P.O. BOX 1663  
LOS ALAMOS, NM 87545 (5 COPIES)

RU SHAN WU  
UNIV. OF CALIFORNIA, SANTA CRUZ  
EARTH SCIENCES DEPT.  
1156 HIGH STREET  
SANTA CRUZ, CA 95064

JAMES E. ZOLLWEG  
BOISE STATE UNIVERSITY  
GEOSCIENCES DEPT.  
1910 UNIVERSITY DRIVE  
BOISE, ID 83725

TERRY WALLACE  
UNIVERSITY OF ARIZONA  
DEPARTMENT OF GEOSCIENCES  
BUILDING #77  
TUCSON, AZ 85721

DANIEL WEILL  
NSF  
EAR-785  
4201 WILSON BLVD., ROOM 785  
ARLINGTON, VA 22230

JIAKANG XIE  
COLUMBIA UNIVERSITY  
LAMONT DOHERTY EARTH OBSERV.  
ROUTE 9W  
PALISADES, NY 10964